A NUMERICAL SIMULATION OF VASCULAR BRAIN TUMOR GROWTH USING ADOMIAN DECOMPOSITION METHOD.

PhD THESIS

BY

WANJAU PAUL MAINA

REG.NO. DPH/AM 04/14

A THESIS SUBMITTED IN PARTIAL FULFILMENT OF THE REQUIREMENTS FOR THE AWARD OF A DEGREE OF DOCTOR OF PHILOSOPHY IN APPLIED MATHEMATICS OF MOI UNIVERSITY, ELDORET KENYA

SEPTEMBER 2017

DECLARATION

Declaration by the Student

I the undersigned declare that this thesis is my original work and has not been presented for academic purposes in this university or any other institution for academic purposes whatsoever.

Signature…… Date……

Paul Maina Wanjau

Recommendation by Supervisors

This Thesis has been submitted for examination with our approval as the university Supervisors.

Signature…… Date……..

Prof. Joseph Kipsigei Koske

Department of Statistics and Computer Science, Moi University, Box 3900-30100 Eldoret, Kenya.

Signature…… Date…….……..

Prof. Francis Kimani Gatheri

School of Mathematics and Acturial Sciences, Technical University of Kenya, Box 52428-00200 Nairobi, Kenya.

ABSTRACT

A tumor develops when a single normal cell transforms due to mutations in certain key genes. To continue growing, it requires new sources of nutrients, hence develops new blood vessels that continue feeding it from the blood leading to vascularization. Statistics from World Health Organization (WHO) records shows that incidences of brain tumors in the year 2014 were already at 1/12,500 persons. The purpose of this study was to develop a numerical simulation of vascular brain tumor that will help medical practitioners to predict the size of the tumor for prognosis purposes instead of exposing patients to radiations through multiple scanning. In this work numerical simulation was developed from partial differential equations models, whereby cell nutrients concentration(C) was the dependent variable x, y, z were spatial independent variables, t was a variable for different time schedules, P was the variable for cells proliferation, P_n was the variable for non- proliferating cells while N was the variable for necrotic cells. Objectives of study were, to develop a numerical simulation of vascular brain tumor growth in one, two and three dimensions, to determine the viable rate of consumption of the nutrients in tumor growth and development, to present validated results in tabular and graphical form, to determine the period within which angiogenic inhibitors are viable. In attaining the objectives above results were generated by Adomian Decomposition Method (ADM) whereby equations are decomposed into a series of Adomian polynomials. The method generates a solution in the form of a series whose terms are determined by a recursive relationship. Results obtained from the simulation of growth and dynamics of malignant brain tumor (glioma) compares well with those from medical literature. In one dimensional model, radius of the tumor in different time schedules was obtained, for example where the rate of diffusion of the nutrients was 11mm/year, in 560 days, simulation radius was found to be 25.4mm compared to an experimental radius of 25.0 mm. In two dimensional models, cross section area of the tumor in different time schedules was obtained, whereby in 560 days, simulation area was found to be 19.02cm^2, whereas analytical area was 19.64cm^2. In three dimensional models, volume of the tumor in different time schedules was obtained, whereby in 560 days, simulation volume was found to be 65.77cm^3, whereas analytical volume was 65.48cm^3. Thus obtained results were found to be consistent with available experimental data, hence may be used to complement traditional tumor diagnostic. Considering idealized cases of tumors, ADM gave realistic simulations, which can provide clinical practitioners with valuable information on the potential effects of therapies in their exact schedules. However for tumors with multiple distinct clones, current model may not be reliable thus further studies are needed to address this shortcoming.

TABLE OF CONTENTS

LIST OF TABLES

LIST OF FIGURES

LIST OF SOME FUNCTIONS AND PARAMETERS

L	Differential operator
L^{-1}	Integral operator
C	Dependent variable giving the concentration of nutrients
C_0	Dependent variable at 0^{th} Iteration (Initial concentration of the nutrients)
C_n	Dependent variable at n^{th} Iteration.
t	Independent variable representing time
t_i	Time at i^{th} iteration.
A_0	0^{th} Adomian polynomial.
A_n	n^{th} Adomian polynomial.
γ	Parameter used in Adomian polynomial.
φ_n	Approximate solution up to the n^{th} term.
R_t	Average overall tumor radius
δ_p	Proliferative rim thickness which determines the tumor growth fraction
δ_n	Non proliferative thickness which determines necrotic fraction
R_n	Necrotic radius.
D_c	Proportionality constant.

DEDICATIONS

I dedicate this work to my beloved family; my wife Grace and daughters Esther and Josephine My Parent Milka and my entire family. Without your encouragement and support this journey would have been long and tough. You put your heart in all that I did, supported, facilitated, encouraged and prayed for me.

ACKNOWLEDGEMENTS

I sincerely thank the almighty God through the lord Jesus Christ for his divine mercy and provision, without which the dream of completion of this work would not have been realized. I am especially grateful to my two supervisors, Professor Francis Kimani Gatheri of Technical University of Kenya and Professor Joseph Kipsigei Koske of Moi University for their professional guidance and supervision of this project. Their contribution to the study of Numerical Simulation of Vascular Brain Tumor of which their monitoring, motivation and attention throughout this research was the key to the successful completion of this project. My appreciation also goes to Prof. Ambrose Kiprop, Dr. F.O. Nyamwala and all the lecturers in Department of Mathematics and Physics for their co-operation and guidance on matters of academics from the time I enrolled for this program. I also appreciate Professor Bernard Ikua of school of Engineering (JKUAT) for the very positive input, his dedication and also provision of learning materials. Special gratitude goes to Professor Farai Nyabadza who is a senior lecturer in Universiteit-Stellenbosch University in South Africa, Dr Andrew Omandi Cole of centre for Research in Therapeutic Science (Strathmore University), Dr Opondo A. Everisto (Consultant Surgeon- Orthopaedics & Trauma) and also Mr Wilson Mwangi Kabue of Ronalo Medical Centre (Nakuru) for their great contribution towards this work.My special gratitude goes to my wife Grace, my daughters, Esther and Josephine for their immeasurable support and understanding. I deeply appreciate the encouragement and prayers from my Mother Milka. Your moral support made this work a reality.I also wish to appreciate Dr. Muvengei of Engineering department (JKUAT) for the technical assistance and his major contribution towards developing this research work. Special gratitude also goes to my close friend and colleague Cyrus Ngari for his immeasurable input and support. Your deep concern gave me a smooth sailing in this work. I am extremely grateful to my other colleagues: Benson, Martin, Rosemary, Hannah, Kennedy, Kande, Njoki, Florence, Musyoki, and Kairu for their warm company, assistance and suggestions throughout our course on Applied Mathematics. Thank you all and God bless.

CHAPTER ONE

INTRODUCTION

This chapter gives the background information of Adomian Decomposition Method (ADM) and also tumor development from avascular to vascular stage. It also gives the definition of some key terms, problem statement, justification and objectives of this work.

1.0 Background Information

The Adomian decomposition method for solving differential and integral equations linear or non-linear was proposed by the American physicist Adomian (1980). The method has been used to solve effectively and easily a large class of linear and non- linear ordinary and partial differential equations.

It has the advantage of converging to the exact solution and can easily handle a wide class of both linear and non-linear differential and integral equations. It has been found to be efficient since it requires less computational work while still maintaining high accuracy of the numerical solution. Also it has the ability to solve non-linear problems without linearization, has wide applicability to several types of problems in scientific fields since it develops a reliable analytical solution. The method is analytic and requires neither linearization nor perturbation. It can be applied directly for all types of differential and integral equations, linear or nonlinear, homogeneous or inhomogeneous with constant coefficients or with variable coefficients.

In this work results are generated by using Standard Adomian decomposition method (SADM). This method involves separating the equation under investigation into linear and non-linear portions. The linear operator representing the linear portion of the equation is inverted and the inverse operator is then applied to the equation. Any given conditions are taken into consideration. The non-linear portion is decomposed into a series of Adomian polynomials.

This method generates a solution in the form of a series whose terms are determined by a recursive relationship using these Adomian polynomials.

It is fundamental to note that the development of a primary solid tumor begins with a single normal cell becoming transformed as a result of mutations in certain key genes (Friedman, 2006). This transformed cell differs from a normal one in its escape from the body's homeostatic mechanisms, leading to inappropriate proliferation and a tendency to override apoptosis (cell death). An individual tumor cell has the ability over successive divisions to develop into a cluster of tumor cells. Further growth and proliferation leads to the development of an avascular tumor consisting of approximately 10^6cells. A solid tumor may typically be detected only when it attains a radius of 0.5mm, by then it contains about 10^9 cells. At this stage the cells feed on oxygen and other nutrients present in the local environment that is, it is at benign stage. In order to continue growing it requires new sources of nutrients, hence it secretes chemicals called tumor growth factors which stimulate the formation of new blood vessels that continue feeding the tumor from the blood. This is the process of angiogenesis. A tumor which has developed beyond this stage is said to be vascularized. After the early stages of growth, the tumor's structure consists of an inner zone of necrotic cells (dead due to lack of nutrients) and an outer zone of living cells. This outer zone is further divided into a layer composed of non- proliferating cells and a layer largely composed of proliferating cells.

According to WHO, global incidences of primary malignant brain and central nervous system tumors are 3.6 per 100,000 persons per year in males and 2.5 per 100,000 persons per year in females. The incidence rates are higher in more developed countries that is, males; 5.9 per 100,000 persons per year and females: 4.1 per 100,000 persons per year. In less developed

countries males 2.8 per 100,000 persons per year while females' incidences are 2.0 per 100,000 persons per year. This discrepancy may partly be a reflection of poor facilities for diagnosis.

The incidence of malignant brain tumor in the UK is higher than the world average for both men (8.1 per 100,000), and women (5.3 per 100,000). There has been no significant change in these rates over the past 10 years.

In the USA, the rate is 7.6 per 100,000 for men and 5.3 per 100,000 for women. American men have a 1 in 149 lifetime risk of being diagnosed with a primary malignant brain tumor and a 1 in 204 chance of dying from a brain tumor. Women have a 1 in 200 lifetime risk of being diagnosed with a primary malignant brain tumor and 1 in 256 chance of dying from this cause.

The model analyzed here devises a method to provide a reasonably realistic discrete size of a tumor in different time schedules for prognosis purposes.

1.1 Definition of key terms

1.1.1 Stability: A method is said to be stable when obtained solution undergoes small variations as there are slight variations in inputs and parameters.

1.1.2 Adomian decomposition method: This is a series expansion method and is independent of small physical parameters as compared to well known perturbation theory hence giving the method greater flexibility and solution generality.

1.1.3 Perturbation theory: Comprises Mathematical methods that are used to find an approximate solution to a problem which cannot be solved exactly by starting from the exact

solution of a related problem. Perturbation theory is applicable if the problem at hand can be formulated by adding a small term to the mathematical description of the exactly solvable problem, while further terms describe the deviation in the solution due to the deviation from the initial problem.

1.1.4 Primary tumor: The tumor at its initiated location which is traced to a single mutated cell, from which over a period of time a colony of cells is formed.

1.1.5 Benign: Where the mass of abnormal cells remains clustered together and confined to the cavity.

1.1.6 Malignant: Where the tumor has emerged out of the cavity by breaking out through the basal membrane and then proliferating into the extracellular matrix.

1.1.7 Vascular tumor: A tumor which has developed beyond the process of angiogenesis.

1.1.8 Avascular tumor: A tumor in the advanced stage of development. It is approximately 1mm in diameter. It contains approximately 10^6 cells including the normal cells.

1.1.9 Necrotic cells: These are dead cells which cannot be able to multiply. They are found at the inner core of the tumor.

1.1.10 Quiescent cells: Cells which are not yet necrotic but as well cannot proliferate since they do not have an access to the nutrients. Found in the middle core of the tumor.

1.1.11 Proliferating cells: Cells which are actively multiplying since they have an access to the nutrients. Found on the surface of the tumor.

1.1.12 Magnetic Resonance Imaging (MRI) is a procedure in which radio waves and a powerful magnet linked to a computer are used to create detailed pictures of areas inside the body. These pictures can show the difference between normal and diseased tissues.

1.1.13 Tumor angiogenesis: It is the growth of blood vessels between a tumor and its surrounding tissues. New blood vessels help the tumor to grow by feeding the cancer cells with essential nutrients and oxygen.

1.1.14 Neurologic symptoms: Symptoms of disorders that affect the brain and the central nervous systems for example, muscles weakness, decreased alertness, unexplained pain among others.

1.2 Statement of the problem

WHO records show that incidences of brain tumors is already at 8/100,000 persons per year and is still increasing. According to American Brain tumor association's statistics updated in 2014, approximately 4,600 children are diagnosed with a brain tumor in the U.S per year of which 72 percent of these children are younger than 15 years. The Association also estimates that about 700,000 people will be diagnosed with a primary brain tumor in the US every year. Unfortunately, each year about 14,000 people die of brain tumors in the U.S. In less developed countries males' incidences are at 2.8 per 100,000 persons per year while females' are 2.0 per 100,000 persons per year. This discrepancy may partly be a reflection of poor facilities for diagnosis. Substantial progress has been made in the various specialized areas of cancer research, yet the complexity of the disease lead to description of tumors as complex and dynamic. By virtual of being dynamic, patients diagnosed with tumor require immediate medical attention which may sometimes not be affordable or available. Therefore simulation carried out in this work will help medical practitioners to predict the size of untreated tumor for prognosis purposes instead of exposing oncologic patients to radiations through multiple scanning.

1.3 Justification

After understanding the complexity of the tumors, simulations must be developed which incorporates concepts from many scientific areas such as cancer research, applied mathematics and dynamical systems. The simulation carried out in this work is basically meant for predicting the size of tumor at given time schedules after detection. It can help in evaluation of the therapeutic potential of some treatment strategies owing to the size of the tumor.

For patients who are unable to undergo treatment immediately after scanning, medical practitioners can use the simulation to predict the size of the tumor for prognosis purposes in specific time schedules without further scanning hence not exposing patients to radiations through multiple scanning.

1.4 Research Objectives

1.4.1 General objective

To carry out numerical simulation of vascular brain tumor growth from Partial Differential Equations models using Adomian Decomposition Method (ADM).

1.4.2 Specific objectives

(i) To perform numerical simulation of vascular brain tumor growth in one, two and three dimensions.

(ii) To determine the viable rate of consumption of the nutrients in tumor growth and development.

(iii) To present validated results in tabular and graphical form.

(iv) To determine the period within which angiogenic inhibitors are viable.

1.5 Scope of the study

The purpose of this research is to present this new and reliable method (ADM) for solving ordinary and partial differential equations. In presenting this work, the aim is also to test the proposed method in handling a generalization of various types of problems. Specifically this research provides a numerical simulation of vascular brain tumor growth by using the method.

Since its introduction, ADM has been attracting the attention of many mathematicians, physicist and engineers. It has been the subject of extensive analytical and numerical studies. In recent years, a large amount of literature has been developed concerning the method by applying it to large size of applications in applied sciences. Significant research has also been done in the modeling of tumors using theoretical models and computer simulations as outlined in the next chapter.

CHAPTER TWO
LITERATURE REVIEW

2.0 Introduction

In this chapter, some of the earlier work that has been done by researchers in the field of ADM and also tumor modeling using both theoretical models and computer simulations is outlined.

2.1 Adomian Decomposition Method (ADM)

Since its introduction, ADM has been attracting the attention of many mathematicians, physicist and engineers. It has an advantage of converging to the exact solutions and can easily handle a wide class of linear and non- linear differential and integral equations.

It has been the subject of extensive analytical and numerical studies. A large amount of literature has been developed concerning the method by applying it to large size of applications in applied sciences.

It is interesting to point out that a useful comparison between the Adomian decomposition method and the Picard method was conducted by Rach (1987) to show that the two methods are not the same and Picard's method works only if the equation satisfies the Lipschitz condition. Bellomo and Monaco (1985) have shown significant advantages of decomposition method over perturbation techniques. Both studies can be used to formally show that the decomposition method is neither Picard's method nor a form of perturbation techniques.

Related phenomena were recently established to facilitate the convergence of the solution or to make savings in the computational work. Adomian and Rach (1992) introduced and defined the phenomena of noise terms. The noise terms were defined as the identical terms with opposite signs that appear in the first two components of the series solution of u(x). It was concluded that if a term or terms in the component u_0 are cancelled by a term or terms in the

component u_1, even though u_1 contains further terms, then the remaining non- cancelled terms in u_0 may provide the exact solution u(x). It was shown that the noise terms appear always for inhomogeneous equations. This development is proved to be useful in demonstrating a fast convergence of the decomposition series solution.

The theoretical treatment of the convergence of Adomian decomposition method has also been considered in Abbaoui and Cherruault (1995), Hosseini and Nasabzadeh (2006). According to them the solution is found as an infinite series which converges rapidly to accurate solutions. The method has many advantages over the classical techniques; mainly it makes unnecessary the linearization of nonlinear terms, perturbation and other restrictive methods and assumptions.

In his book, Adomian (1994) showed the possibility of obtaining explicit solutions of wide varieties of physically significant problems, for example, he analyzed the mathematical models of the dynamics involved in population of bacteria, viruses, antigens or tumor cells. These models are usually nonlinear hence their solution generally begins by some form of linearization or perturbation. He found that the method is independent of linearization, perturbation as well as discretization hence greatly reducing the CPU time.

Wazwaz (1997) developed a necessary condition that is essentially needed to ensure the appearance of noise terms in the inhomogeneous equations. The necessary conditions for the noise terms to appear in the components u_0 and u_1 are that the exact solution u(x) must appear as part of u_0 among other terms. In addition, the remaining non- cancelled terms of $u_0$must satisfy the equation under discussion.

The new necessary condition developed by Wazwaz (1997) was formerly proved and tested to demonstrate the power of the noise terms whence these terms appear in the components u_0 and u_1.

A new modification was proposed by Wazwaz (1999) which demonstrated a rapid convergence of the series solution compared to the standard Adomian method and therefore presented a major progress. This modified decomposition method has been showed to be computationally efficient in several examples that are important to researchers in applied fields. In addition the modified decomposition method may give the exact solution by using two iterations only and without using Adomian polynomials. In this modification, the modified form was established based on the assumption that the function f (x) can be divided into two parts namely $f_0(x)$ and $f_1(x)$. Under this assumption, we set

$$f(x) = f_0(x) + f_1(x) \quad \text{.....(2.1)}$$

Accordingly a slight variation was proposed only on the component u_0 and u_1. The suggestion was that only the part f_0 be assigned to the zeroth component u_0 whereas the remaining part f_1 be combined with the other terms to define u_1. Consequently the modified recursive relation was developed i.e.

$$u_0 = f_0(x)$$

$$u_1 = f_1(x) - L^{-1}(Ru_0) - L^{-1}(A_0),$$

$$u_2 = -L^{-1}(Ru_1) - L^{-1}(A_1),$$

$$u_{k+2} = -L^{-1}(Ru_{K+1}) - L^{-1}(A_{k+1}), k \geq 0, \quad \text{.....(2.2)}$$

Where L is the highest order term which is assumed to be easily invertible and R is the remainder of the linear operator. Ru_0 represent the remainder of linear operator at 0^{th} iteration while Ru_{k+1} represents the remainder of linear operator at $(k+1)^{th}$ iteration. A is the nonlinear operator at different iterations. Comparing the recursive scheme of the standard Adomian method

That is,

$$u_0 = f(x)$$

$$u_1 = -L^{-1}(Ru_0) - L^{-1}(A_0),$$

$$u_{k+1} = -L^{-1}(Ru_k) - L^{-1}(A_k), k \geq 0 \text{..... ....} (2.3)$$

The recursive scheme above of modified decomposition method leads to the conclusion that in equation (2.3),the zeroth component was defined by a function $f(x)$. Whereas in equation (2.2) , the zeroth component $u_0(x)$ was defined only by a part $f_0(x)$ of $f(x)$.

The remaining part $f_1(x)$ of $f(x)$ is added to the definition of the component $u_1(x)$ in equation (2.3).The slight variation in reducing the number of terms of u_0 reduced the size of the computation work. Further, because of the dependence of the Adomian polynomials of the zeroth components $u_0(x)$ in non-linear equations, the reduction of terms in u_0 produced a reduction in the size of calculations. Furthermore, the slight variation in the definition of the components u_0 and u_1 may provide the solution by using two iterations only. However the success of the modified decomposition method depends entirely on the proper selection of functions f_0 and f_1. Wazwaz (1999) also noted that modified method does not always minimize the size of calculations needed and even requires much more calculations than the standard Adomian method.

Wazwaz, and El-sayed (2001) proposed the two step Adomian decomposition method (TSADM) to modify the standard Adomian decomposition method and make further progress beyond the achievement made so far in this regard.

The TSADM may provide the solution by using one iteration only compared with the standard Adomian method and the modified method.

A comparative study between the TSADM and the modified decomposition method is conducted to illustrate the efficiency of the TSADM. Comparing the standard Adomian method and the modified method, it can be seen that the TSADM may provide the solution by using one iteration only. Furthermore, the number of terms in f is small in many practical problems.

Chen *et al.*(2004) established an algorithm that can be easily programmed and be used to calculate Adomian polynomials for nonlinear terms in the differential equations. The basic goal is to mechanize the computation of the decomposition method by maple program, so that we can obtain the approximate solutions conveniently. However, though the program always provides effective analytical solutions in this field, there are some open problems about the Adomian decomposition method such as the general convergence of

$$\sum_{n=0}^{\infty} u_n \text{..... ....} (2.4)$$

and the error estimation of the approximate solution

$$u_n = \sum_{i=0}^{n-1} u_i \text{..... ....} (2.5)$$

So he observed that the results produced by the program should be dealt with carefully.

Aminataei and Hosseini (2007) compared the stability of Adomian decomposition method with other numerical methods. In comparison with the solution obtained by using the finite difference method, the conclusion was that Adomian decomposition method is weaker in stability than finite differences but stronger in convergence.

The general conclusion was that Adomian decomposition method, despite its greater efficiency in solving differential equations suffers certain weaknesses.

Liu (2009) used the orthogonal polynomials to modify the Adomian decomposition method. The method of employing Legendre and Chebyshev polynomial to improve the Adomian decomposition method was presented in his paper, he concluded that both orthogonal polynomials; Chebyshev and Legendre can be successfully used to improve the Adomian decomposition method and the obtained approximated solution is more accurate than the one obtained through regular ADM. Comparatively, Chebyshev polynomials provides better estimation than Legendre polynomials. According to him the partial sums of Chebyshev expansion of a continuous function on [-1,1] converge faster than those of any other polynomials, however he observed that Legendre polynomials were superior because of unit weight function and hence easier for application.

Biazar *et al*. (2009), extracted a general iterative method from an Adomian decomposition method and compared it to the variation iteration method. They achieved this goal and presented a general iteration formula which seems to be effective. In conclusion, the two methods led to the results which were exactly the same; hence they recommended that the method be used for solving other functional equations.

Kumar and Singh (2010) presented an efficient numerical algorithm for solving singular two-point linear and non-linear problems which is based on the modified Adomian decomposition method (MADM). Also they proposed a new operator for solving singular boundary value problems (BVPS) which gives lesser error compared to MADM and other existing techniques given in the literature.

The method successfully worked to give very reliable and accurate solutions to the singular problem. The method gives convergent approximations and handles non-linear problems. In this method, there is no need for linearization of nonlinear terms.

For nonlinear problems, MADM is seen to be a very good choice to achieve a high degree of accuracy while dealing with both linear and nonlinear problems.

Adomian decomposition method is implemented directly in a straight forward manner without using restrictive assumptions. Comparing the results with other existing methods it has been proved that MADM is a more powerful method for solving various kinds of singular boundary value problems.

Also comparing MADM with the finite difference method (FDM), cubic Spline method, MADM is less stable than finite differences and other methods but has a better convergence. It can be concluded that MADM has a greater convergence in solving singular boundary value problems.

The new method is also not much affected by computational round off errors and there is no necessity of large computer memory and time, compared with the FDM and other methods.

Emad *et al.*(2011), advanced the ADM for solving two- point nonlinear boundary value problems with Neumann boundary conditions. The aim of their work was to introduce a direct approach for solving ordinary and partial second order boundary value problems with

Neumann boundary conditions. This extension is based on a new definition of the inverse linear operator. The main advantage of this approach is the direct way of dealing with the Neumann boundary conditions.

In addition, a unique solution results or a class of approximate solutions is otherwise obtained. The ADM is validated by discussing several linear and nonlinear ordinary and partial two point boundary value problems. It is shown that, for a sufficiently small number of components the approximate and exact solutions become nearly identical.

Emad *et al.*(2012) developed a new straight forward approach for solving ordinary and partial second-order boundary value problems with Neumann boundary conditions. This approach depends mainly on the Adomian decomposition method with a new definition of the differential operator and its inverse, which has been modified for Neumann boundary conditions. The effectiveness of the proposed approach is verified by several linear and nonlinear examples.

Wanjau *et al.*(2016) Compared the convergence of ADM and that of fourth order Runge Kutta method by applying them in obtaining a numerical simulation of Third order Ordinary differential equation. According to the results obtained ADM has a better convergence than fourth order Runge Kutta method.

Significant research has also been done in the modeling of tumors using theoretical models and computer simulations. Previous modeling has been done on a range of tumor behaviors, including proliferative growth of tumor core.

2.2 Tumor Modeling

Some of the earliest work in modeling of tumors using a three dimensional cellular automaton on a cubic lattice was carried out by Dutching and Vogelsaenger (1985) for very small tumors. These automaton rules were designed to reflect nutritional needs for tumor growth.

Other important factors, such as surrounding cells and mechanical pressure, however, remained unconsidered.

Adam (1986) used an ordinary differential equation to model the growth of the tumor which reflected mass conservation of tumor cells, coupled with a reaction-diffusion equation. His main interest was about the distribution of nutrients within the tumor. He found that the distribution of nutrients within the tumor is basically governed by fluid dynamics principles.

Qi et al. (1993) considered a two dimensional cellular automaton tumor model. However, cells could only divide if one of their nearest neighbors was empty; this created an unrealistically small fraction of tumor which may divide. Furthermore, dead tumor cells were assumed to simply dissolve away rather than accumulating into a necrotic core, as is seen in real tumors.

Smolle and Stettner (1993) showed that the macroscopic behavior of a tumor can be affected by the presence of growth factors at the microscopic level and added the concept of cellular migration to the behavior of the cells. However, their work was qualitative and designed to show the range of behaviors obtainable from a simple model.

Chiocca *et al.*(2000) developed a three dimensional cellular automaton model which describes tumor as a function of time. The algorithm takes into account that growth starts out from a few cells, passes through a multi cellular tumor spheroid (MTS) stage and proceeds to the

macroscopic stages. According to their work an idealized case of a tumor is essentially spherical within a small degree of randomness. However, their algorithm gave simulation on only four designated time points i.e. spheroid stage, detectable lesion, diagnosis and death. Their algorithm could not provide information about the rate of diffusion of the nutrients within the proliferative rim of the tumor.

Nicholson (2001) considered diffusion and related transport mechanisms in brain tissue. He highlighted the role of diffusion in brain function. According to him, the spaces between cells can be likened to the water phase of foam and many substances move within this complicated region.

Diffusion in this space can be accurately modeled with appropriate modifications of classical equations. Besides delivering glucose and oxygen from the vascular system to the brain cells, diffusion also moves informational substances between cells, a process known as volume transmission. Diffusion is also essential to many therapies that deliver drugs to the brain.

Cheng (2005) developed a mathematical model for the quantitative description of the dynamics of avascular tumor growth. The model was formulated as a set of partial differential equations describing the spatial-temporal changes in cell concentrations based on reaction-diffusion dynamics and the law of mass conservation. His model was solved using standard finite difference techniques. He observed that even though the results compared well with those of experimental data, they could only be obtained at discrete points depending on the step sizes provided. This created a shortcoming since tumor growth is a dynamic process.

Friedman (2006) presented generic PDE models which governs the growth and development of tumors. He observed that the tumor region is a three dimensional region $\Omega(t)$ which varies

with time (t).Within $\Omega(t)$ there are several types of cells as well as several different chemicals such as oxygen and other nutrients. The densities of the cells and the concentration of the chemicals satisfy a system of partial differential equations. However a major difficulty in the analysis of the models was due to the fact that the region $\Omega(t)$ is one of the unknowns hence becoming a free boundary problem. By being generic models he never specified the parameters and hence never obtained the simulation.

Friedman (2013) developed a partial differential equation model of the growth and response to treatment of prostate cancer. He considered existence and uniqueness of solutions for proven radially symmetric case. Finally, numerical simulations of a tumor growing in two dimensions with radial symmetry were carried out in order to evaluate the therapeutic potential of different treatment strategies.

The simulations were able to reproduce a variety of clinically observed responses to treatment and suggested treatment strategies that may result in tumor remission, underscoring the model's potential to make a significant contribution in the field of prostate cancer therapeutics. He proved that for tumor cell growth rate the tumor radius was not consistent but had oscillatory behavior.

Konukoglu et al (2010) defined gliomas as tumors arising from glial cells of the central nervous system (CNS).According to them, they form an invasive class of tumors with poor prognosis following their Anaplastic transformation. A severe impediment to their treatment is the diffuse and heterogeneous rate of invasion that leads to invisible outer tumor, undetectable under current imaging resolutions. This heterogeneous pattern of spread has

partly been attributed to the anisotropic invasion of glioma cells along aligned structures in the brain, such as the bundled neural fibre tracts characteristics of white matter.

Hillen and Painter (2013); presented a model of glioma invasion along the aligned neural fibre tracts. According to them, the invasion is facilitated by the directed movement of cells along the aligned neural fibre tracts that form a large component of the white matter. Diffusion Tensor Imaging (DTI) provides a window for visualizing this anisotropy and gaining insight on the potential invasive pathways. They demonstrated the results in a simple model for glioma growth exploiting both synthetic and genuine DTI datasets to reveal the potentially crucial role of anisotropic structure on invasion.

Naveja *et al*. (2014) presented a model which was stated upon fundamental assumptions to produce a predictor of the clinical outcomes of patients undergoing a tumor resection. They used an ODE model validated for predicting the immune system response and the tumor growth in oncologic patients.

The model could be further extended to a personalized prognosis predictor and tools for improving therapeutic strategies.

In this work a model of vascular primary brain tumor is developed and its numerical simulation obtained using Adomian decomposition method. The method has an advantage in that it does not require discretization or linearization of nonlinear problems.

Chapter three below gives the model formulation as well as the step by step description of Adomian Decomposition Method.

CHAPTER THREE

METHODOLOGY AND MODEL FORMULATION

3.0 Introduction

This chapter outlines the procedure for ADM which facilitate development of the simulation for the models. The section as well outlines the steps of model formulation based on information obtained from WHO records.

3.1 Application of Adomian decomposition method in obtaining a numerical simulation of vascular brain tumor growth.

Fluid dynamics often give rise to non-linear differential equations. These problems end to be more difficult to solve, often with no known exact solution. As such researchers are continually looking for ways to accurately and efficiently solve these problems.

Many methods have been developed to solve the non-linear differential equations, but there is need for a method which requires high accuracy with lower number of iterations.

In this work standard numerical method was developed and applied in solving a nonlinear PDE model governing the diffusion of nutrients in the tumor. This new algorithm is derived from the standard Adomian decomposition method (ADM) so as to present an alternative to such classic schemes as the explicit Runge-Kutta methods for engineering and biological models.

Under this method, the model is separated into linear and nonlinear portions. The linear operator representing the linear portion of the equation is inverted and the inverse operator is then applied to the equation. Initial conditions for tumor growth and development are taken

into consideration. The nonlinear portion is decomposed into a series of Adomian polynomials.

This method generates a solution in the form of an infinite series which converges to accurate solutions. Also there is graphical representation of the solution for the purposes of better comparison and analysis.

3.2 Description of the method

In describing the ADM, we consider the general equation $F\varphi = g$,

Where F represents a general nonlinear differential operator involving both linear and nonlinear terms, the linear term is decomposed into L+R where L is easily invertible and R is the remainder of the linear operator. For convenience, L may be taken as the highest order derivative. Thus the equation may be written as;

$$L\varphi + R\varphi + N\varphi = g \quad \text{.....(3.1)}$$

Where $N\varphi$ represents the nonlinear terms and g is the source term.

Solving $L\varphi$ from equation 3.1 we have;

$$L\varphi = g - R\varphi - N\varphi \quad \text{.....(3.2)}$$

Because L is invertible, the equaivalent expression is

$$L^{-1}L\varphi = L^{-1}g - L^{-1}R\varphi - L^{-1}N\varphi \quad \text{.....(3.3)}$$

If L is a third order differential operator, then L^{-1} is a three fold integral operator and hence

Computing left hand side of (3.3) yields;

$$L^{-1}L\varphi = \varphi - \varphi(0) - \varphi'(0)t - \varphi''(0)\frac{t^2}{2} \quad \text{.....(3.4)}$$

The equation 3.4 for φ yields

$$\varphi = \varphi(0) + \varphi'(0)t + \varphi''(0)\frac{t^2}{2} + L^{-1}g - L^{-1}R\varphi - L^{-1}N\varphi \quad \text{.....(3.5)}$$

Or

$$\varphi = a + bt + ct^2 + L^{-1}g - L^{-1}R\varphi - L^{-1}N\varphi \quad \text{.....(3.6)}$$

Where

$a = \varphi(o)$, $b = \varphi'(0)$, $c = \varphi''(0)$

Therefore φ, which is dependent variable can be presented as a series, that is

$$\varphi = \sum_{n=0}^{\infty} \varphi_n$$

.....(3.7)

The nonlinear term Nφ will be decomposed by the finite series of Adomian polynomials

$$N\varphi = \sum_{n=0}^{\infty} A_n$$

.....(3.8)

Where A'_ns are obtained by writing

$$\varphi(\gamma) = \sum_{n=0}^{\infty} \gamma^n \varphi_n$$

……..(3.9)

$$N[\varphi(\gamma) = \sum_{n=0}^{\infty} \gamma^n A_n$$

……(3.10)

Where γ is a parameter introduced for convenience.

A_n's are Adomian polynomials that can be constructed for various classes of non – linearity.

Whereby

$$A_0 = F(\varphi_0)$$

$$A_1 = \varphi_1 F'(\varphi_0)$$

$$A_2 = \varphi_2 F'(\varphi_0) + \varphi_1^2 \tfrac{1}{2} F''(\varphi_0)$$

$$A_3 = \varphi_3 F'(\varphi_0) + \varphi_1 \varphi_2 F''(\varphi_0) + \varphi_1^3 \tfrac{1}{3!} F'''(\varphi_0)$$

.

$$A_n = \tfrac{1}{n!} \frac{d^n}{d\gamma^n} \left\{ F\left(\sum_{i=0}^{n} \gamma^i \varphi_i \right) \right\}_{\gamma=0 \quad n=0,1,2.....} \quad \text{……(3.11)}$$

Where F represents a general nonlinear differential operator and φ_0 is the dependent variable at 0^{th} iteration. φ_1 is the dependent variable at first iteration among others.

Hence taking $\varphi_0 = a + bt + ct^2 + L^{-1}g$ and substituting equations (3.7) and (3.8) into equation (3.6);

we obtain

$$\sum_{n=0}^{\infty}\varphi_n = \varphi_0 - L^{-1}R\sum_{n=0}^{\infty}\varphi_n - L^{-1}\sum_{n=0}^{\infty}A_n \quad \text{.....(3.12)}$$

consequently, we can write

$$\varphi_0 = a + bt + ct^2 + L^{-1}g$$

$$\varphi_1 = -L^{-1}R\varphi_0 - L^{-1}A_0$$

$$\varphi_2 = -L^{-1}R\varphi_1 - L^{-1}A_1$$

$$\varphi_{n+1} = -L^{-1}R\varphi_n - L^{-1}A_n \quad \text{.....(3.13)}$$

Whereby

$$\varphi = \sum_{n=0}^{\infty}\varphi_n \quad \text{.....(3.14)}$$

The series converges since, $\lim_{n\to\infty}\varphi_n \to 0$

$$\phi(t) = \varphi_0 + \varphi_1 + \varphi_2 + .. + \varphi_{n+1} \quad \text{.....(3.15)}$$

For PDEs

L = $\frac{\partial^n}{\partial t^n}$. Hence

$$Lu = g - Ru - Nu \quad \text{.....(3.16)}$$

where L is the highest order derivative and R is the remainder of the linear operator, N represents nonlinear terms.

L^{-1} Operator, which is a multiple integral from 0 to t (that is definite integral within a specific time schedule), is then operated on equation (3.16) to yield:

$$L^{-1}Lu = L^{-1}g - L^{-1}Ru - L^{-1}Nu \quad \text{……..……...(3.17)}$$

The left side of equation (3.17) will be obtained as:

$$L^{-1}Lu = u - Q_t$$

……..……(3.18)

Where $Q_t = u(0) + u^{'}(0)t + u^{''}(0)\frac{t^2}{2}$. From equations (3.17) and (3.18), we can write:

$$u = Q_t + L^{-1}g - L^{-1}Ru - L^{-1}Nu \quad \text{…….....(3.19)}$$

Suppose the answer to equation (3.16) is as follows:

$$u = \sum_{n=0}^{\infty} u_n$$

……...……...…….(3.20)

Then, the substitution of equation (3.20) for equation (3.19) will yield:

$$u = \sum_{n=0}^{\infty} u_n = Q_t + L^{-1}g - L^{-1}R\sum_{n=o}^{\infty} u_n - L^{-1}N\sum_{n=0}^{\infty} u_n \quad \text{……..……..……...(3.21)}$$

Where

$$Q_t = u(0) + u^{'}(0)t + u^{''}(0)\frac{t^2}{2}$$

Consequently;

$$u_o = Q_t + L^{-1}g,$$

$$u_{n+1} = -L^{-1}Ru_n - L^{-1}Nu_n(n \geq 0) \quad \text{.....(3.22)}$$

From (3.22), the series can be generated as,

$$u_o = Q_t + L^{-1}g,$$

$$u_1 = -L^{-1}Ru_0 - L^{-1}f(u),$$

$$u_2 = -L^{-1}R(-L^{-1}Ru_0 - L^{-1}f(u)) - L^{-1}f(u),$$

$$u_3 = -L^{-1}R((-L^{-1}R)^2u_0 + (L^{-1}R)L^{-1}f(u) - L^{-1}f(u)) - L^{-1}f(u),$$

$$= (-L^{-1}R)^3u_0 - (L^{-1}R)^2(L^{-1}f(u)) + L^{-1}R(L^{-1}f(u)) - L^{-1}f(u),$$

$$= (-1)^3(L^{-1}R)^3u_0 + \sum_{k=0}^{2}(-1)^{k+1}(L^{-1}f(u)$$

$$u_n = (-1)^n(L^{-1}R)^nu_0 + \sum_{k=0}^{n-1}(-1)^{k+1}(L^{-1}R)^kL^{-1}f(u) \quad \text{.....(3.23)}$$

$$u_{n+1} = (-1)^{n+1}(L^{-1}R)^{n+1}u_0 + \sum_{k=0}^{n}(-1)^{k+1}(L^{-1}R)^kL^{-1}f(u) \quad \text{.....(3.23)}$$

$$u = u_0 + u_1 + u_2 + \ldots\ldots\ldots\ldots + u_n \quad \text{.....(3.24)}$$

3.3 Model Formulation.

Information obtained from WHO records indicate that a tumor (also called a neoplasm or lesion) is abnormal tissue that grows by uncontrolled cell division. Normal cells grow in a controlled manner as new cells replace old or damaged ones. For reasons not fully understood, tumor cells reproduce uncontrollably. Basically brain tumor is a mass of abnormal cells growing in the brain, that is;

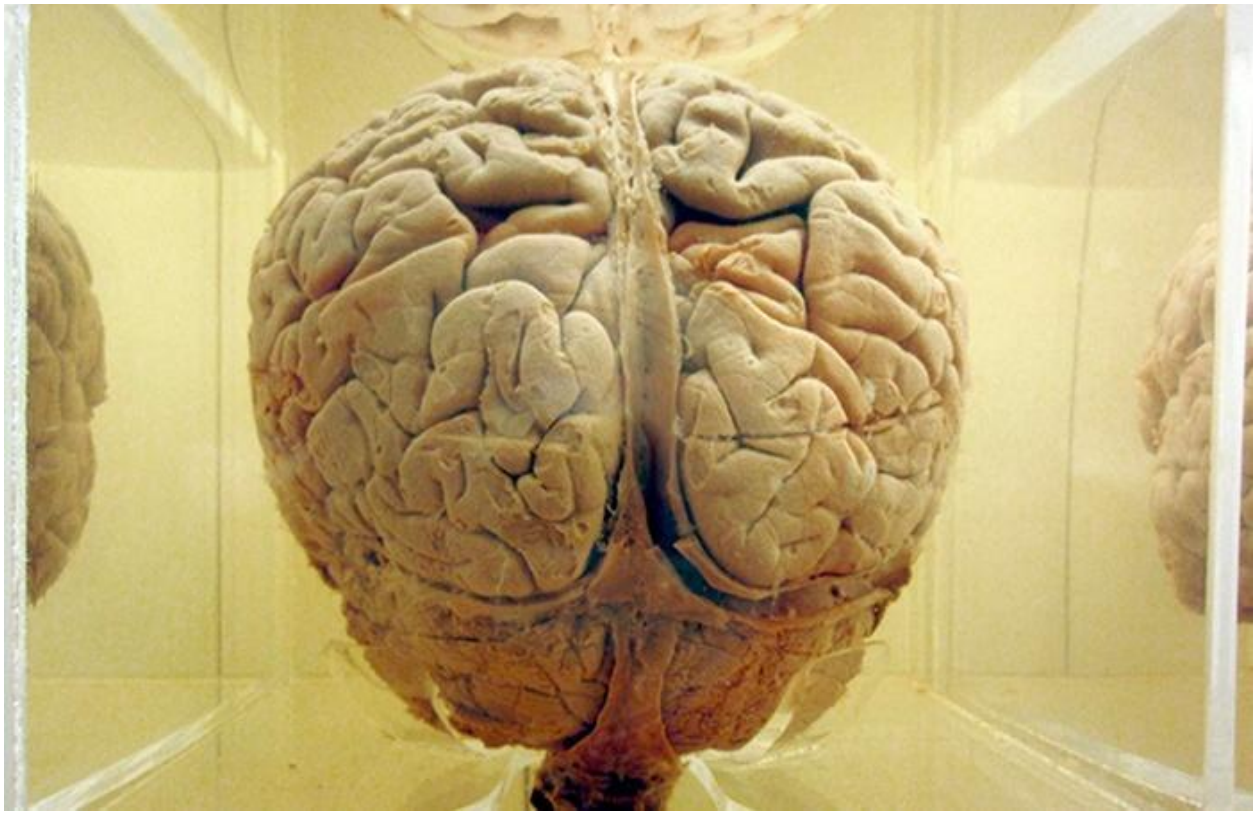

Fig. 3.1;3-Dimensional brain tumor geometry by Francisco Jose Torres -2015

It compresses and displaces normal brain tissues applying pressure on the tissues hence causing neurologic symptoms.

The figures below show images of brain tumors at different positions of the brain or for patients undergoing certain forms of medication.

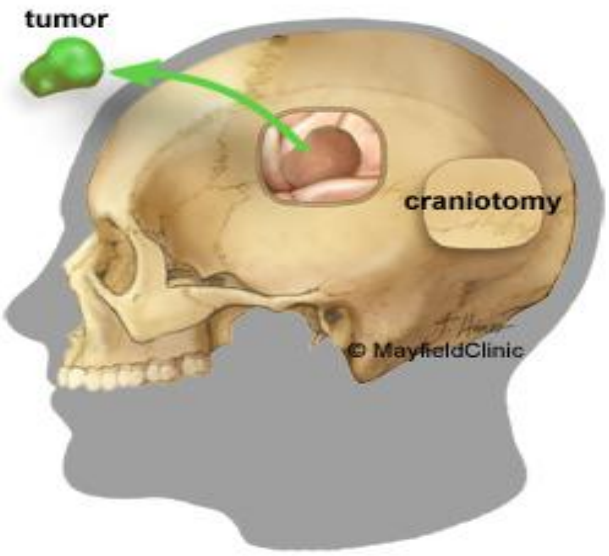

Fig.3.2; Shows a brain tumor of a patient undergoing resection which involves cutting a window in the skull (craniotomy) to remove the tumor**.**

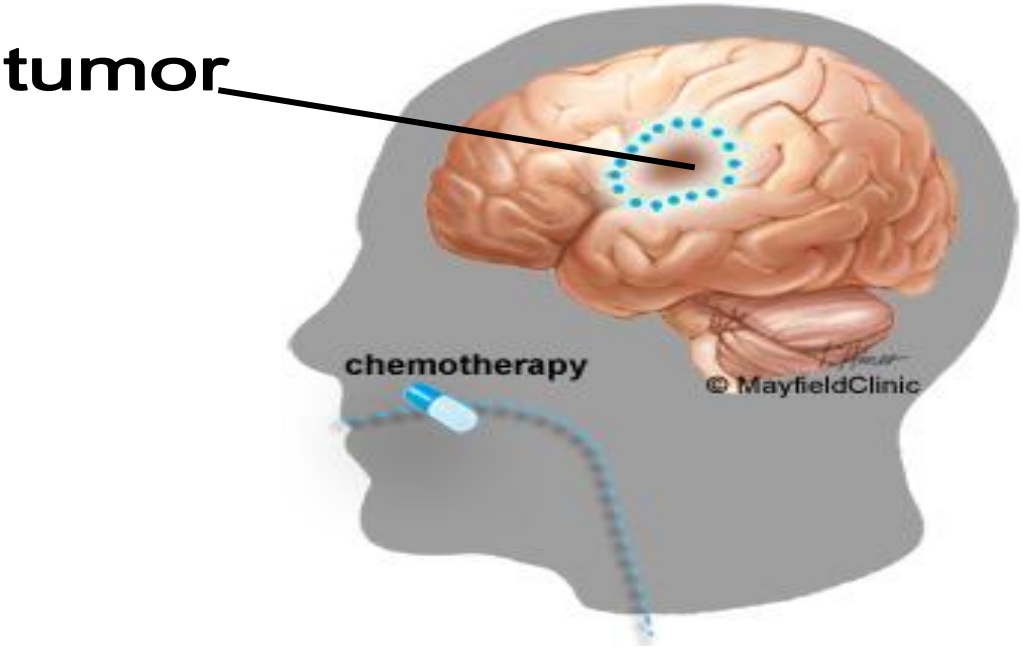

Fig.3.3: Chemotherapy for high-grade glioma. From the website of Mayfield clinic.

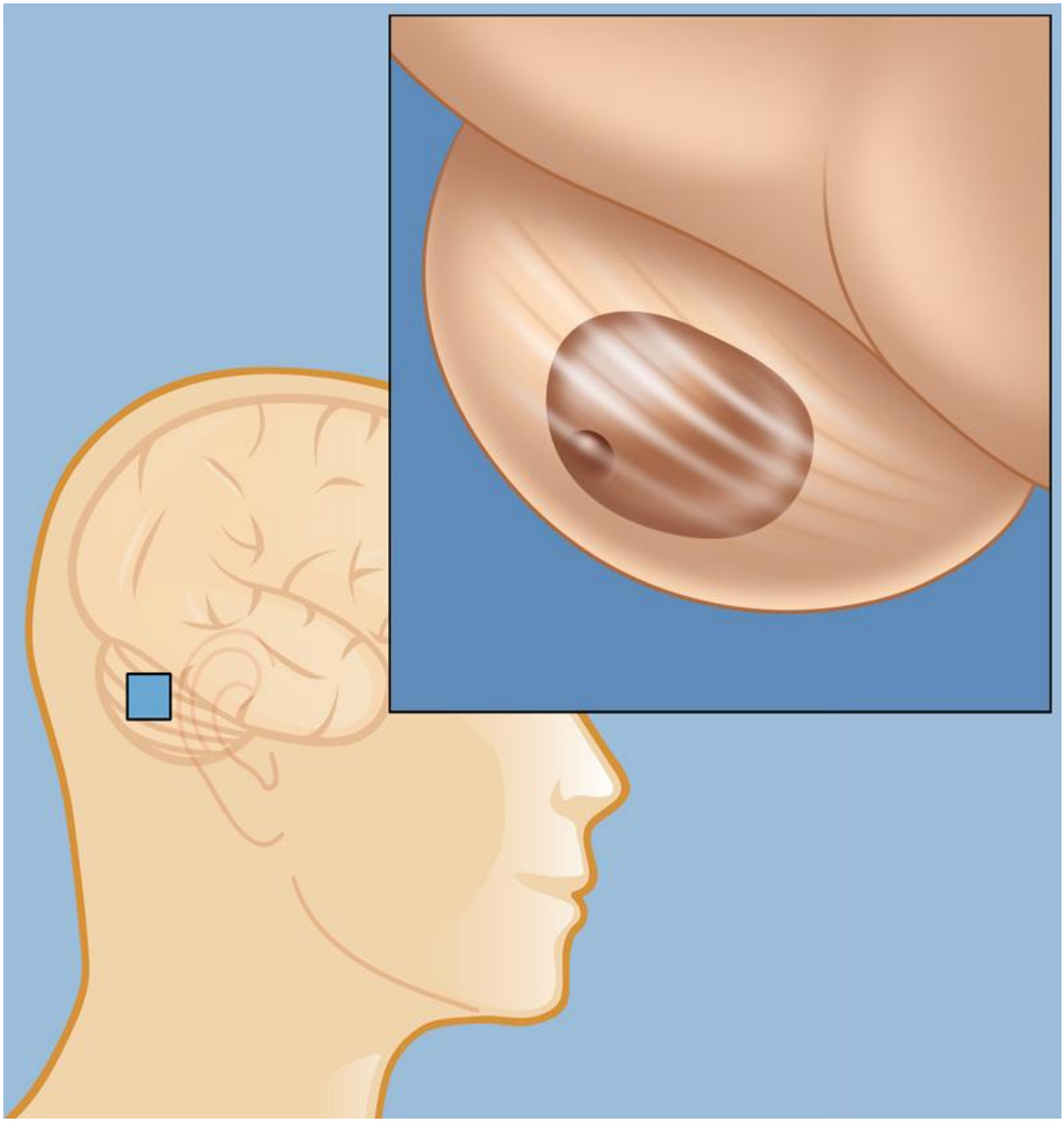

Fig. 3.4: Vascular brain tumor that typically develops in the cerebellum, at the back of the brain, from the website of Weill Cornel Medical College.

Brain tumors are named after the cell of origin. They may be primary (starting in the brain) or secondary (spreading to the brain from another area). They may also be classified according to the behavior of the cells that is their aggressiveness in the process of mitosis. The least aggressive brain tumor is said to be benign while the most aggressive is said to be malignant. Tumors are also classified as Grade I through Grade IV. The more aggressive and dangerous the tumor is, the higher the grade.

Grade I: Also called Pilocytic Astrocytoma. It grows slowly and has well-defined borders, occurs most often in children and teens, accounts for only two percent of all brain tumors.

Grade II: Also called Low-grade Astrocytoma. It grows slowly and is Common among men and women in their 20s to 50s.

Grade III: Also called Anaplastic Astrocytoma. It grows faster and more aggressive than grade II astrocytomas. It is Common among men and women in their 30s to 50s and accounts for two percent of all brain tumors.

Grade IV: Also called Glioblastoma (GBM)**.** It is the most common, accounting for about 50% of all brain tumors. Most fatal of malignant primary brain tumors in adults and is one of a group of tumors referred to as gliomas. Has a Median survival rate of 15 months. Grows faster and is more aggressive than grade III one.

Benign brain tumors are not cancerous but malignant ones are cancerous. Treatment options vary depending on the tumor type, size, location, whether the tumor has spread, age and medical health of the person.

The following figures show the diagrammatic representation of the two types of brain tumors.

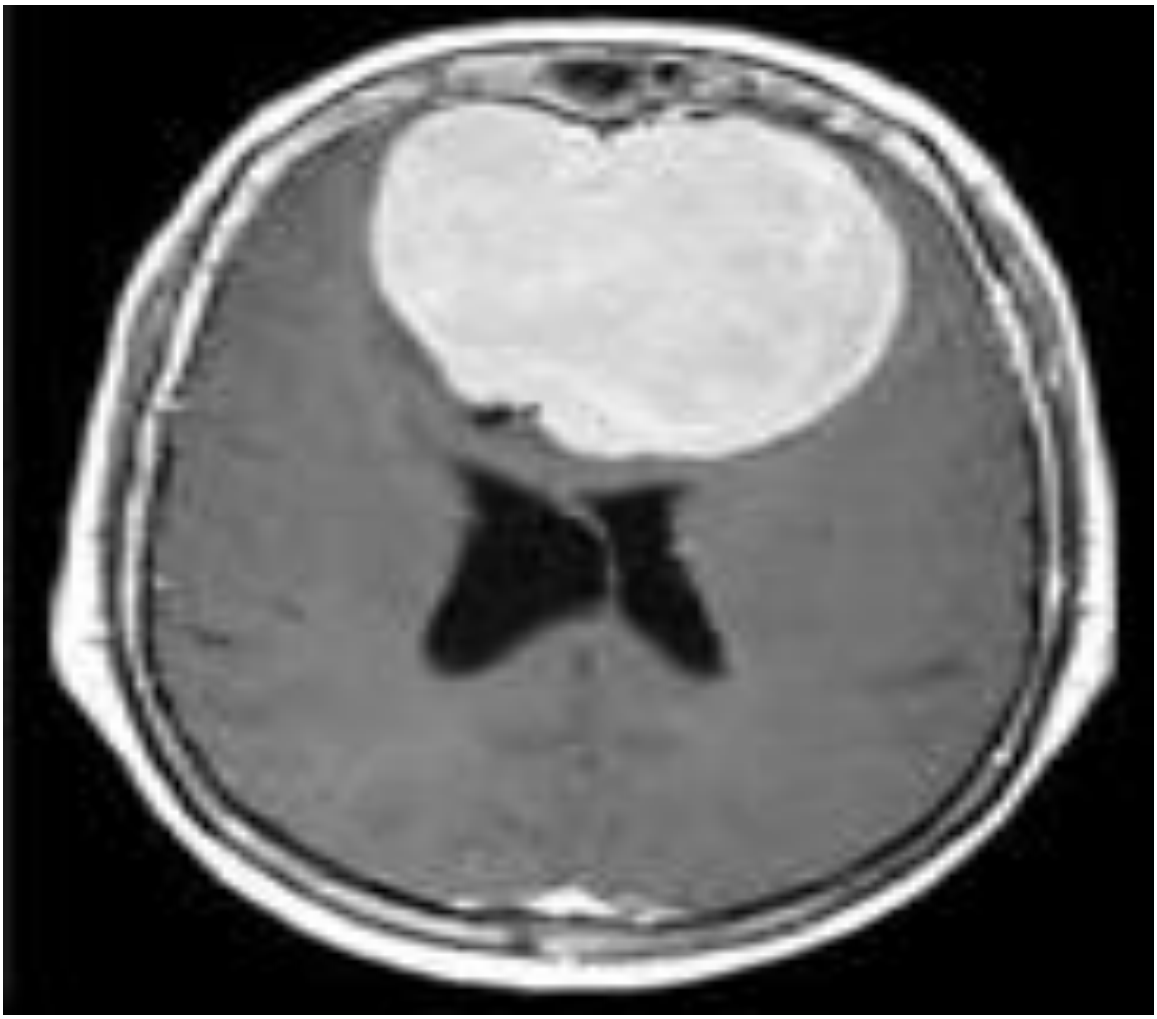

(a)

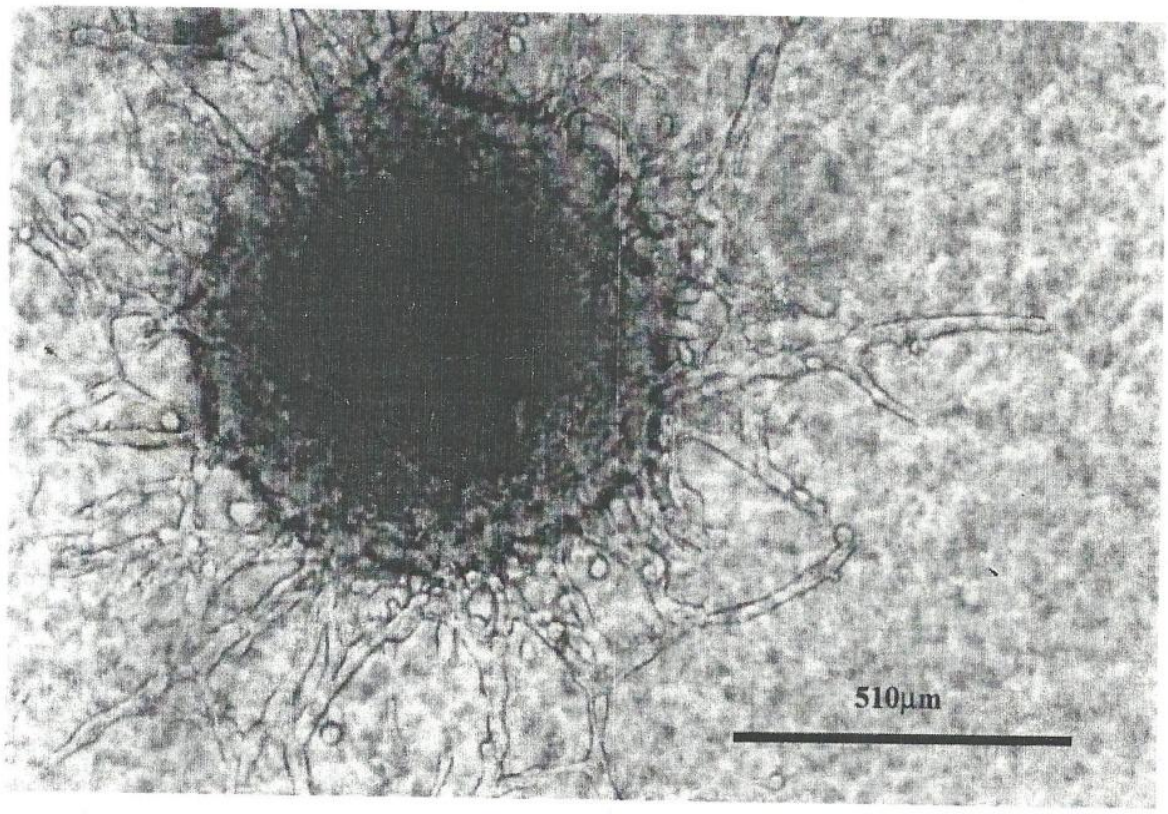

(b)

Fig.3.5: MRI scans of benign (a) and malignant (b) brain tumors.

Benign tumors have well defined edges and are more easily removed surgically. Malignant tumors have an irregular border that invades normal tissue with finger-like projections.

In this work the model of malignant brain tumor (glioma) is considered since it is the most common type as it accounts for about 50 per cent of malignant brain tumors. The simulation is compared with available experimental data for an untreated GBM tumor from medical literature.

In model development we consider the suggested model in Sheralt and Chaplain (2001) for the interaction between the proliferating and non-proliferating (quiescent) cells, namely

$$\frac{\partial}{\partial x}\left[\frac{P}{P+P_n}\frac{\partial(P+P_n)}{\partial x}\right] and \frac{\partial}{\partial x}\left[\frac{p_n}{P+P_n}\frac{\partial(P+P_n)}{\partial x}\right] \quad \text{.....(3.25)}$$

The figure below shows interaction between the different tumor cells.

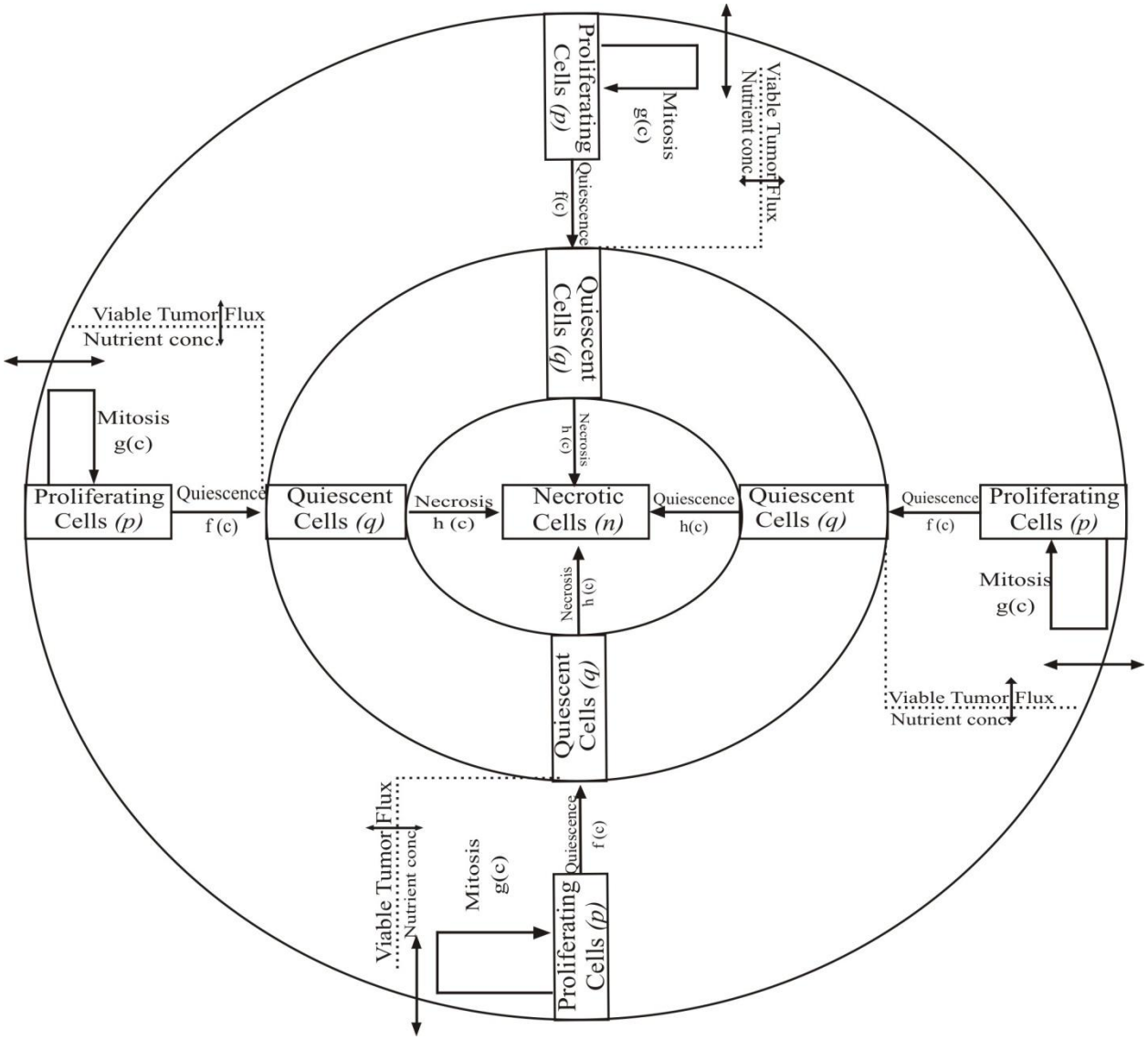

Fig.3.6:A schematic diagram for the interaction between the proliferating, non- proliferating and necrotic cells.

Where P are the Proliferating cells and P_n are non- proliferating (quiescent) cells.

Interactions between different tumor cells give different regions of a tumor reflecting an ideal case as shown in the diagram below.

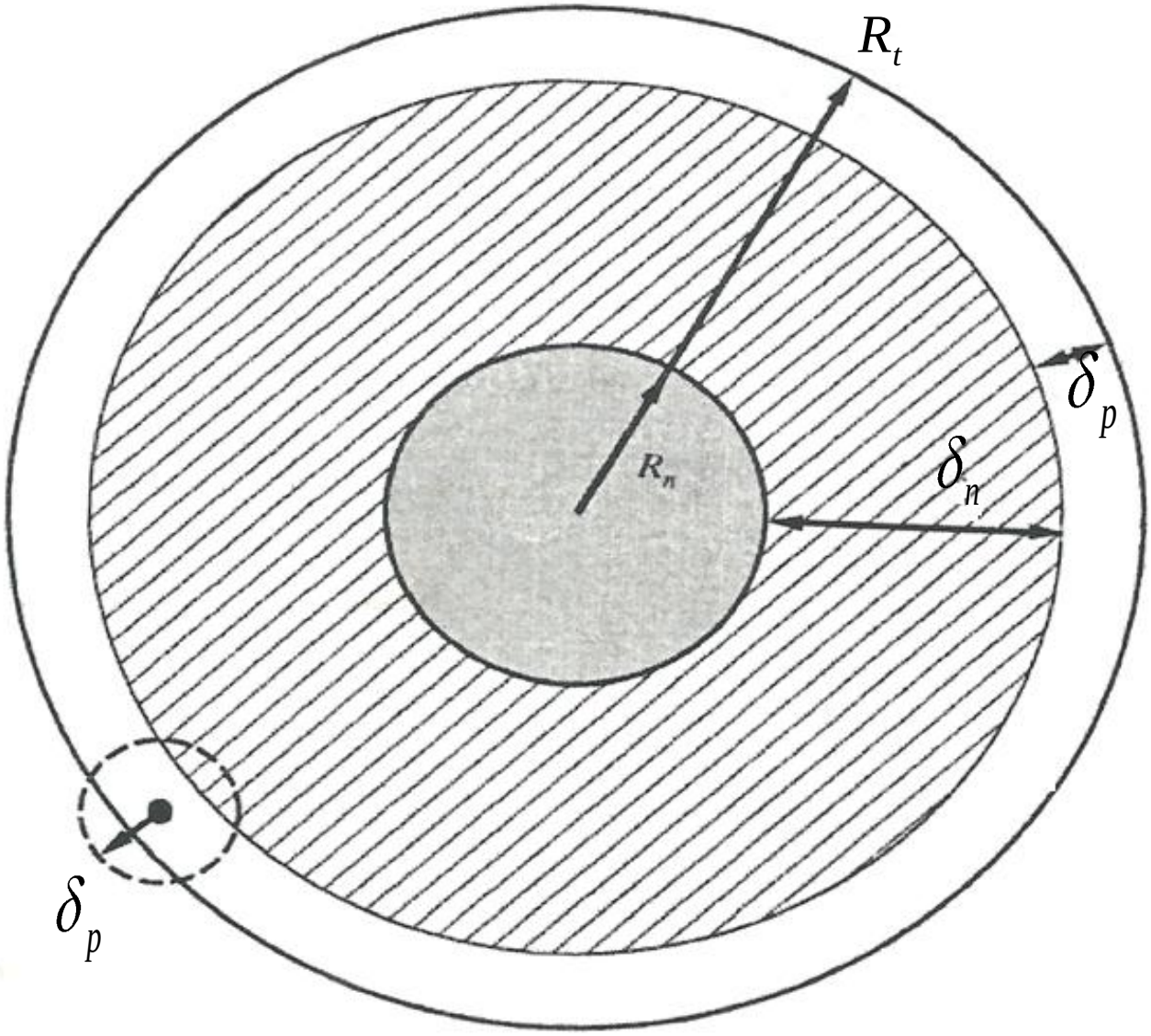

Fig.3.7: A detailed description of different regions of a tumor by Chiocca et al (2000)

A detailed description of different regions of a tumor where;

R_n represents the necrotic region which is a function of time (t).

δ_n is the distance from the proliferating rim to the necrotic region. It represents the region of

Non-proliferative cells.

R_t represents the entire radius of the tumor.

δ_p the distance from the edge of the tumor to non-proliferative cells i.e. the proliferative region.

NB: an individual cell only divide if free space exists within a certain distance of it. This distance must also be represented by δ_p.

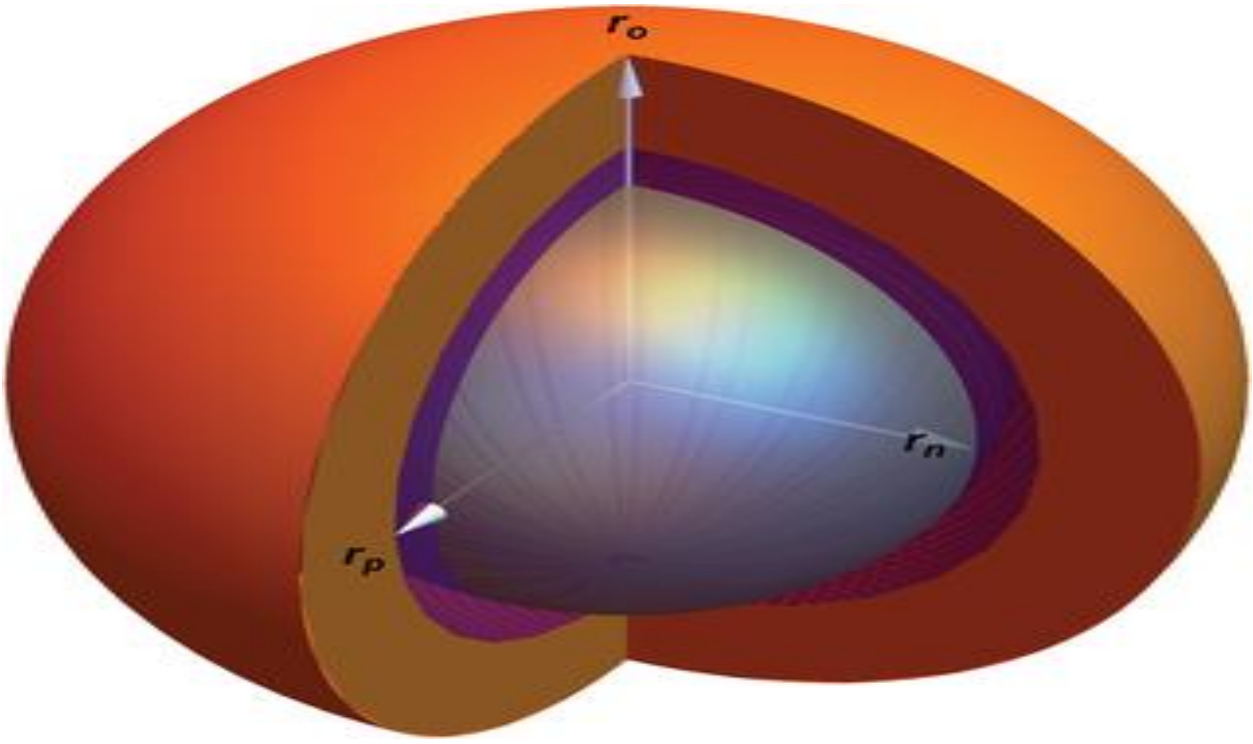

Fig. 3.8: An ideal tumor by Grimes et al (2016) where r_0 is the tumor radius, r_n represents the necrotic radius while r_p represents the radius from necrotic to non-proliferating rim.

The figures below indicate a real tumor developing over a period of time;

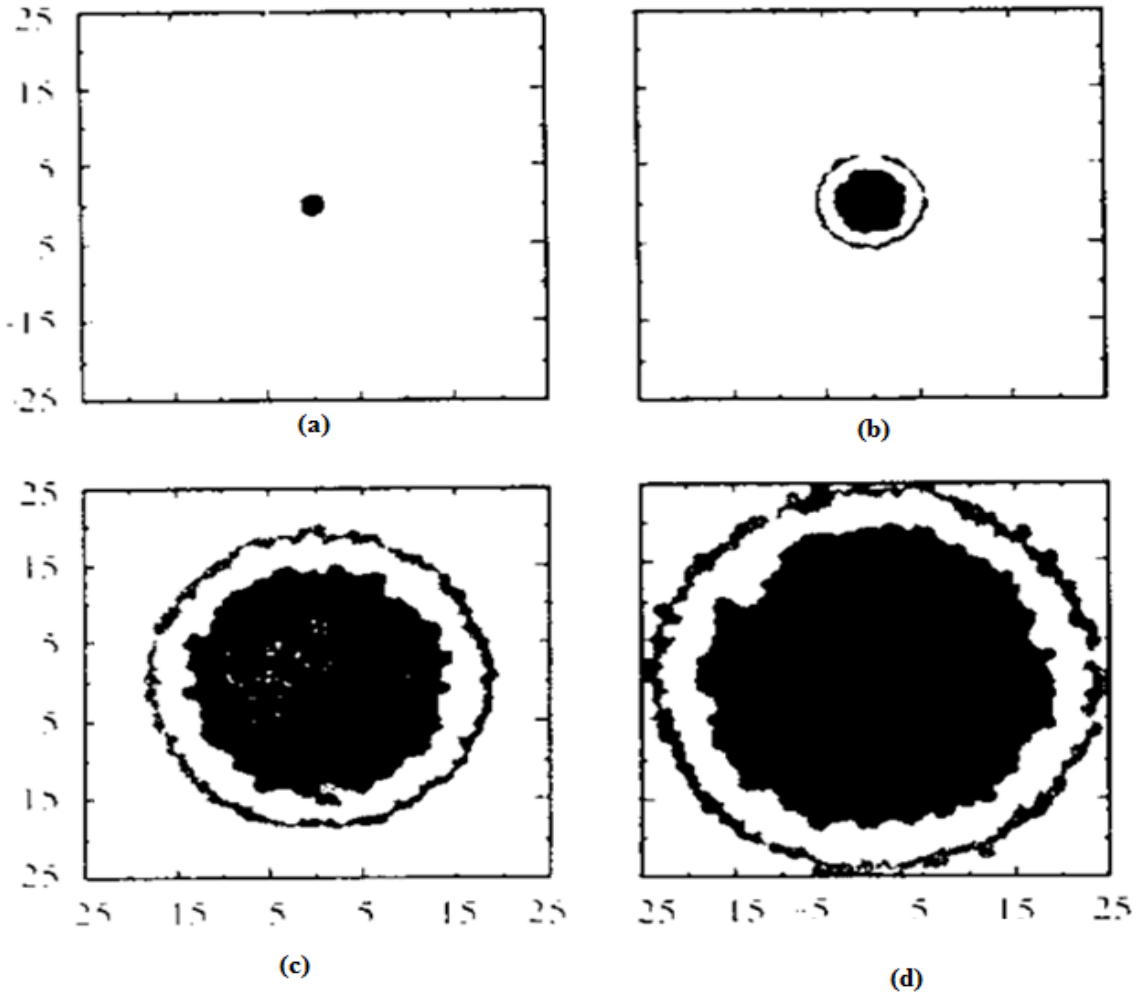

Fig.3.9: The development of the cross-central section of a tumor in time.

(a) Tumor spheroid at approximately 69 days (b) Detectable lesion at approximately 223 days (c) Diagnosis stage at approximately 454 days (d) Fatal stage at approximately 560 days.

The black outer region is comprised of proliferating cells, the white region is non-proliferative cells and the black inner region is necrotic cells. The scales are in millimeters. Chapter four below gives the numerical results, graphical representation and the discussion for the models.

CHAPTER FOUR
RESULTS AND DISCUSSION

4.0: Introduction

This chapter gives the simulation procedure, results and discussion for one, two and three dimensional models. Analysis of the results is done through tabular and graphical representation.

4.1: One dimensional model.

This section gives the simulation procedure, results and discussion for one dimensional model which provides the tumor radius at selected time points. Results obtained are validated by experimental data obtained from WHO medical records. With mass conservation applied to the cells, the set of equations governing the evolution of proliferating, non- proliferating, necrotic cells densities, {Sheralt and Chaplain (2001)} and also nutrients access from underlying tissues in one dimension ,{Friedman (2006)} can be developed as;

$$\frac{\partial P}{\partial t} = \frac{\partial}{\partial x}\left[\frac{P}{P+P_n}\frac{\partial (P+P_n)}{\partial x}\right] + aP - fP - gP. \quad \text{.....(4.1)}$$

$$\frac{\partial P_n}{\partial t} = \frac{\partial}{\partial x}\left[\frac{P_n}{P+P_n}\frac{\partial (P+P_n}{\partial x}\right] + fP - hP_n \quad \text{.....(4.2)}$$

$$\frac{\partial n}{\partial t} = hP_n. \quad \text{.....(4.3)}$$

$$\frac{\partial C}{\partial t} = D_C \frac{x^2 \partial^2 C}{\partial x^2} + \lambda f(x) \quad \text{.....(4.4)}$$

Where:

aP : reprsents mitosis rate of the proliferating cells

fP: represents the rate at which proliferating cells becomes non – proliferative

gP: represents the growth retardation rate

hp_n: represents the rate at which non-proliferative cells which are completely deprived of nutrients undergo necrosis.

Equation (4.4) represents the access of nutrients from underlying tissues.

This is the equation of interest in this work, whereby

D_C and λ are positive constants and $f(x)$ is a source term which is a non-linear function depending on location x. $\lambda f(x)$ is the nutrients consumption rate in one dimension. Proportionality constant (D_C) is approximated as a ratio of 1 hour/ 1 day, a day being taken as a period of approximately 24 hours, hence the exact model for simulation in one dimension becomes;

$$\frac{\partial C}{\partial t} = \frac{x^2}{24}\frac{\partial^2 C}{\partial x^2} + \lambda x^4. \quad \text{.....(4.5)}$$

$f(x)$ is taken as x^4 for integral convenience since a lower index for $f(x)$ will trivialize the source term thus trivializing the polynomial which may results to tumor avasculature. Thus from (4.5),

$$C_t(x,t) = \frac{x^2}{24}C_{xx} + \lambda x^4 \quad \text{.....(4.6)}$$

Where $C(x,0) = 0$ is the initial condition, that is, at $t = 0$, technically it is assumed that there is no spheroid. Thus applying the inverse operator L^{-1} to both sides of equation (4.6) yields;

$$C_0(x,t) = \lambda x^4 t \quad \text{.....(4.7)}$$

$$C_1(x,t) = \frac{1}{24} L_t^{-1}\{x^2 (C_0)_{xx}\}$$

$$= \frac{\lambda}{4} x^4 t^2 \quad \text{.....(4.8)}$$

$$C_2(x,t) = \frac{1}{24} L_t^{-1}\{x^2 (C_1)_{xx}\}$$

$$= \frac{\lambda}{24} x^4 t^3 \quad \text{.....(4.9)}$$

$$C_3(x,t) = \frac{1}{24} L_t^{-1}\{x^2 (C_2)_{xx}\}$$

$$= \frac{\lambda}{192} x^4 t^4 \quad \text{.....(4.10)}$$

$$C_4(x,t) = \frac{1}{24} L_t^{-1}\{x^2 (C_3)_{xx}\}$$

$$= \frac{\lambda}{1920} x^4 t^5 \quad \text{.....(4.11)}$$

$$C_5(x,t) = \frac{1}{24} L_t^{-1}\{x^2 (C_4)_{xx}\}$$

$$= \frac{\lambda}{23040} x^4 t^6 \quad \text{.....(4.12)}$$

$$C_6(x,t) = \frac{1}{24} L_t^{-1}\{x^2 (C_5)_{xx}\}$$

$$= \frac{\lambda}{322,560} x^4 t^7 \qquad \text{……(4.13)}$$

$$C_7(x,t) = \frac{1}{24} L_t^{-1}\{x^2 (C_6)_{xx}\}$$

$$= \frac{\lambda}{5,160,960} x^4 t^8 \qquad \text{……(4.14)}$$

$$C_n(x,t) = \frac{1}{24} L_t^{-1} x^2 (C_{n-1})_{xx} \qquad \text{……(4.15)}$$

Model (4.6) generates the solution in a series of the form;

$$C(x,t) = C_0(x,t) + C_1(x,t) + C_2(x,t) + C_3(x,t) + C_4(x,t) + \ldots\ldots\ldots\ldots C_n(x,t)$$

Whereby

$$\lim_{n\to\infty} C_n(x,t) \to 0 \qquad \text{……(4.16)}$$

Therefore from equation (4.7) to (4.15), the solution in a series form is given by;

$$C(x,t) = \lambda x^4 (t + \frac{t^2}{4} + \frac{t^3}{24} + \frac{t^4}{192} + \frac{t^5}{1920} + \frac{t^6}{23040} + \frac{t^7}{322560} + \frac{t^8}{5160960} - - - - - - - \qquad \text{……(4.17)}$$

Where $C(x,t)$ is the level of nutrients concentration in one dimension which gives the radius of the tumor. λx^4 is the rate of nutrients consumption which is assumed to be directly proportional to the rate of tumor expansion. Chaplain *et al* (1994) estimated $\lambda = 1$ for vascular tumors and $\lambda = 0$ for avascular tumors while spatial variable x^4 is held as unity since tumor

vasculature is assumed to commence at approximate radius of 1cm. In this work λx^4 is approximated as $1.0 cm/year$ and t is variable for time at selected points, equation (4.17) generates the results given in the tables below.

The table below gives the results for one dimensional model at $\lambda x^4 = 10 mm / year$

Results generated from equation (4.17) alongside the ones obtained from medical literature are as tabulated below.

Table 4.1: Comparison between experimental and simulation radius at $\lambda x^4 = 10 mm / year$

Time In years	***Experimental Radius(mm)***	***Simulation Radius (mm)***	***Absolute Error (mm)***	***%(Error/Experimental Radius)***
0.611	*5.0*	*7.2*	*2.2*	*44.0*
0.685	*8.0*	*8.2*	*0.2*	*2.5*
0.767	*10.5*	*9.4*	*1.1*	*10.5*
0.849	*12.0*	*10.5*	*1.5*	*12.5*
0.945	*13.5*	*12.1*	*1.4*	*10.4*
1.027	*15.0*	*13.5*	*1.5*	*10.0*
1.137	*16.5*	*15.3*	*1.2*	*7.3*
1.244	*18.5*	*17.3*	*1.2*	*6.5*
1.389	*22.0*	*20.1*	*1.9*	*7.8*
1.534	*25.0*	*23.1*	*1.9*	*7.6*
1.712	*30.0*	*27.1*	*2.9*	*9.7*

Fig. 4.1: Experimental and simulation radius against time in years at $\lambda x^4 = 10 mm / year$.

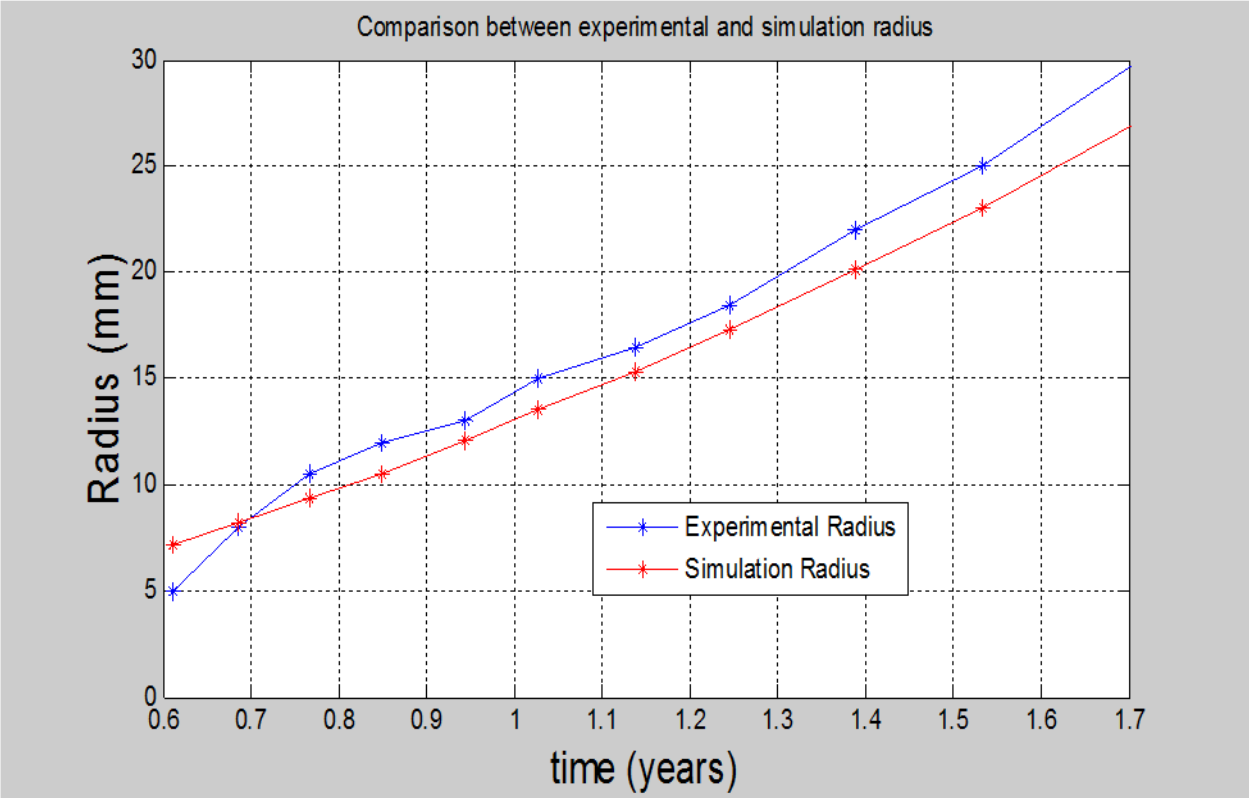

Table 4.1 gives the comparison between experimental and simulation radius when the rate of nutrients consumption is assumed to be 10mm/year. Friedman (2006) noted that, a primary tumor can grow up to a typical size of 1mm without requiring new supply of nutrients, that is it is at benign stage, hence reaction-diffusion model cannot provide a viable simulation at the initial stages of tumor growth and development. At this stage the spheroid does not require new supply of nutrients and is said to be avascular. He also noted that a solid tumor can typically be detected only when it attains a diameter of 1cm.Table 4.1 above gives the simulation of a tumor at selected time points from the detectable level. At this stage tumor has a very high rate of growth which can be attributed to the presence of enough space for cells proliferation. This explains the sharp rise in the test case immediately after detection.

The model provides realistic results for only one selected point that is during the initial levels but unrealistic results in the latter part of growth and development of the spheroid, hence 10mm/year is not a viable rate of nutrients consumption in the entire life of tumor growth and development. Rate of nutrients consumption which is less than or equal to 10mm/year is therefore not viable in this reaction-diffusion process.

Fig 4.1 gives the plots of experimental and simulation radius versus time in years where the rate of nutrients consumption is assumed to be 10mm/year. There is no convergence and hence 10mm/year is not a viable rate of nutrients consumption within this duration of tumor growth and development.

The table below gives the results for one dimensional model at $\lambda x^4 = 11mm/year$

By slightly raising the rate of nutrients consumption to $11mm/year$ then results generated from equation (4.17) alongside the ones obtained from medical literature are as tabulated below.

Table 4.2: Comparison between experimental and simulation radius at $\lambda x^4 = 11mm/year$

Time in years	***Experimental Radius(mm)***	***Simulation Radius (mm)***	***Absolute Error (mm)***	***%(Error/ Experimental radius)***
0.611	*5.0*	*7.9*	*2.9*	*58.0*
0.685	*8.0*	*9.0*	*1.0*	*12.5*
0.767	*10.5*	*10.3*	*0.2*	*1.9*
0.849	*12.0*	*11.6*	*0.4*	*3.3*
0.945	*13.5*	*13.3*	*0.2*	*1.5*
1.027	*15.0*	*14.8*	*0.2*	*1.3*
1.137	*16.5*	*16.8*	*0.3*	*1.8*
1.244	*18.5*	*19.0*	*0.5*	*2.7*
1.389	*22.0*	*22.1*	*0.1*	*0.5*
1.534	*25.0*	*25.4*	*0.4*	*1.6*
1.712	*30.0*	*29.8*	*0.2*	*0.7*

Fig. 4.2: Experimental and simulation radius against time in years at $\lambda x^4 = 11mm / year$.

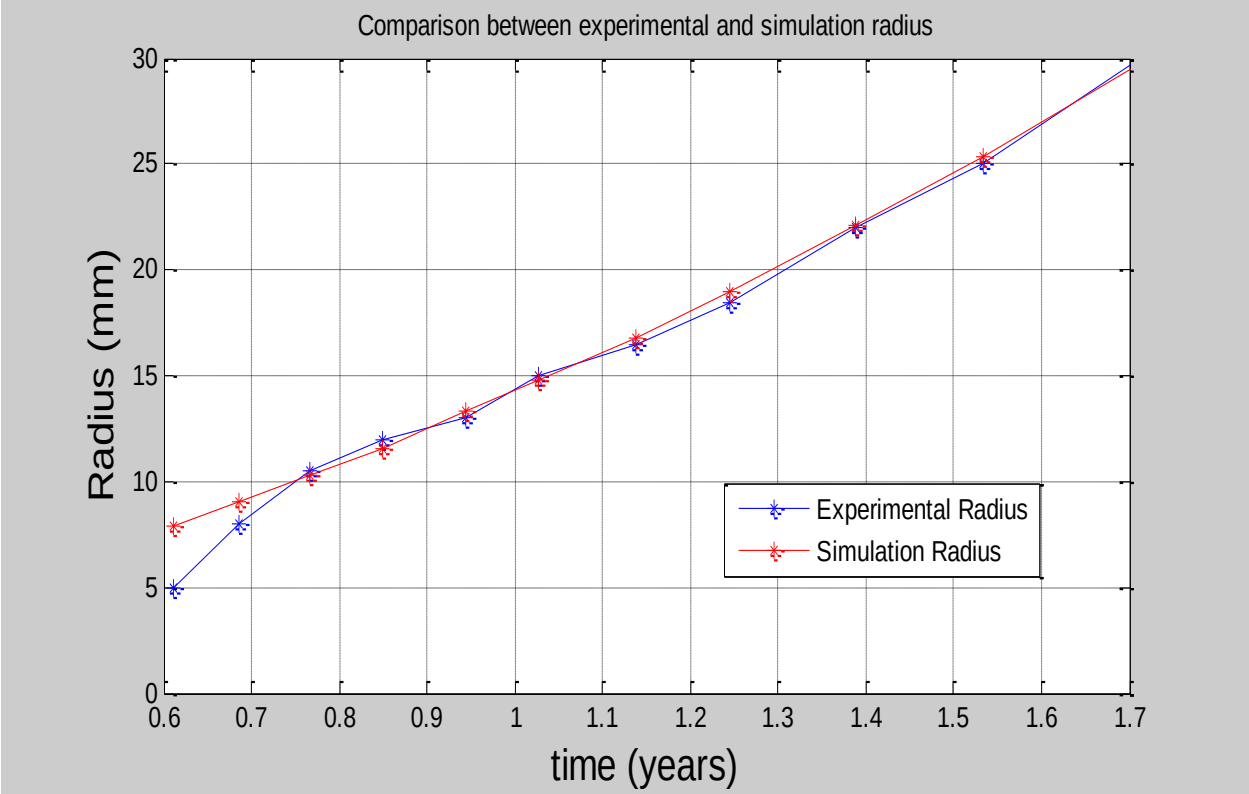

Table 4.2gives the comparison between experimental and simulation radius when the rate of nutrients consumption is assumed to be 11mm/year. Apart from the very initial levels of tumor detection, it can be observed that results are very realistic since they compare well with the experimental ones and hence reaction-diffusion model is viable.11mm/year is the viable rate at which the tumor consumes the nutrients in this reaction-diffusion model. Friedman (2013) noted that for tumor cell growth rate, the tumor radius was not consistent but had oscillatory behavior which is also noted in this simulation.

Fig. 4.2 gives the plots of experimental and simulation radius (in mm) versus time in years. Apart from the initial stages of growth and development of a tumor, there is good convergence between experimental and simulation curves.

The table below gives the results for one dimensional model at $\lambda x^4 = 12 mm / year$

Taking $\lambda x^4 = 12 mm / year$ as the rate of nutrients consumption while t is variable for different time schedules (in years), then results generated from equation (4.17) alongside the ones obtained from medical literature are as tabulated below.

Table 4.3; Comparison between experimental and simulation radius at $\lambda x^4 = 12 mm / year$

Time in years	***Experimental Radius(mm)***	***Simulation Radius (mm)***	***Absolute Error (mm)***	***% (Error/ Experimental Radius)***
0.611	*5.0*	*8.6*	*3.6*	*72.0*
0.685	*8.0*	*9.8*	*1.8*	*22.5*
0.767	*10.5*	*11.2*	*0.7*	*6.7*
0.849	*12.0*	*12.7*	*0.7*	*5.8*
0.945	*13.5*	*14.5*	*1.0*	*7.4*
1.027	*15.0*	*16.1*	*1.1*	*7.3*
1.137	*16.5*	*18.3*	*1.8*	*10.9*
1.244	*18.5*	*20.7*	*2.2*	*11.9*
1.389	*22.0*	*24.1*	*2.1*	*9.5*
1.534	*25.0*	*27.7*	*2.7*	*10.8*
1.712	*30.0*	*32.5*	*2.5*	*8.3*

Fig. 4.3: Experimental and simulation radius against time in years a $\lambda x^4 = 12mm / year$

.

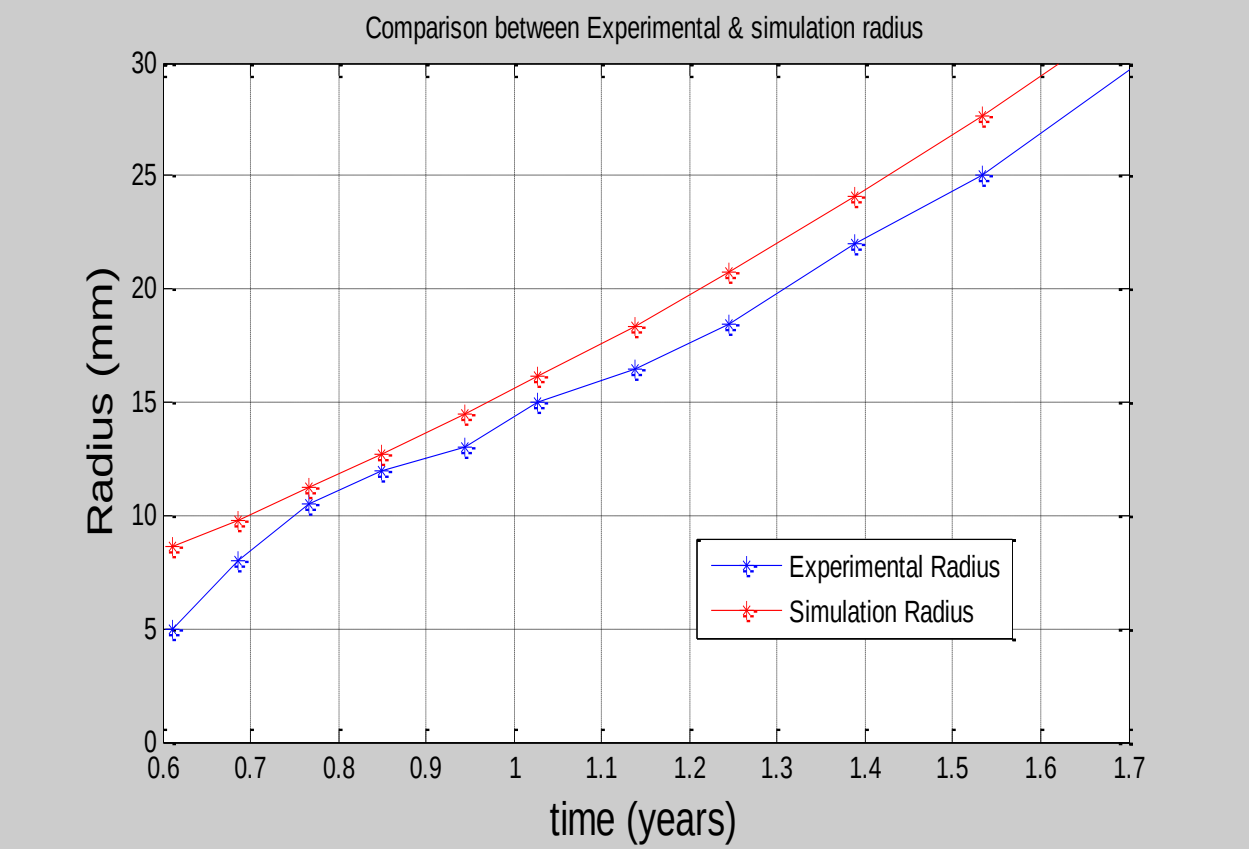

Table 4.3: gives comparison between experimental and simulation radius where the rate of nutrients consumption is assumed to be 12mm/year. The error associated with simulation increases hence rate of nutrients consumption which is greater or equal to 12mm/year is not viable in growth and development of a tumor within this duration.

Fig. 4.3: gives the plots of experimental and simulation radius in mm versus time in years. Since the results obtained from the selected time points fail to compare well, then there is weaker convergence between the two curves. Due to higher rate of consumption of nutrients, the results obtained from selected time points are also high.

In order to obtain the results in months, equation (4.4) need to be formulated as;

$$\frac{\partial C}{\partial t} = \frac{x^2}{720} C_{xx} + \lambda x^4 \quad \text{……..……...…….……..……..(4.18)}$$

Where proportionality constant (D_C) is approximated as a ratio of 1 hour/ 1 month, a month being taken as a period of approximately 30 days.

Solving equation (4.18) by ADM provide equation (4.19) below

$$C(x,t) = \lambda x^4 (t + \frac{t^2}{120} + \frac{t^3}{21600} + \frac{t^4}{5.184 \times 10^6} + \frac{t^5}{1.5552 \times 10^9} + \frac{t^6}{5.59872 \times 10^{12}} + \text{.....} \quad \text{…..…(4.19)}$$

Results generated from equation (4.19) and ones obtained from medical literature are as tabulated.

Table 4.4: Comparison between experimental and simulation radius in Months.

Time in Months	***Experimental Radius(mm)***	***Simulation Radius (mm)***	***Absolute Error (mm)***	***%(Error/ Experimental Radius)***
8.2	*8.0*	*9.7*	*1.6*	*21.2*
9.2	*10.5*	*10.9*	*0.4*	*3.8*
10.2	*12.0*	*12.2*	*0.2*	*1.7*
11.3	*13.5*	*13.6*	*0.1*	*0.7*
12.3	*15.0*	*15.0*	*0.0*	*0.0*
13.6	*16.5*	*16.8*	*0.3*	*1.8*
14.9	*18.5*	*18.6*	*0.1*	*0.5*
16.6	*22.0*	*21.0*	*1.0*	*4.5*
18.4	*25.0*	*23.7*	*1.3*	*5.2*
20.5	*30.0*	*26.9*	*3.1*	*10.3*

Fig.4.4: Experimental and simulation radius against time in Months.

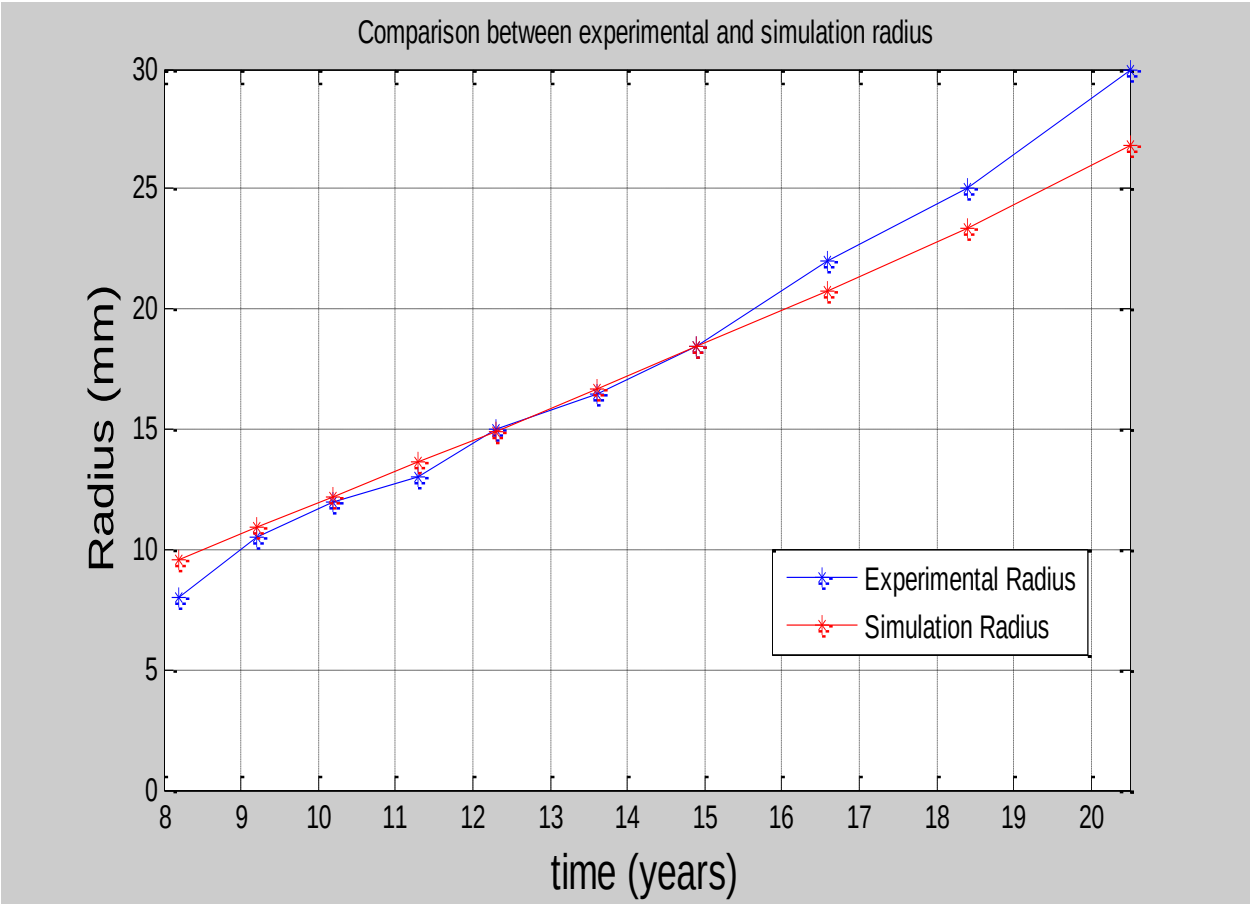

Table 4.4 gives comparison between experimental and simulation radius in months. Even though the simulation provides good results at some points, it can generally be observed that results provided do not compare well with experimental ones. This can be attributed to the fact that results provided in months are highly affected by rounding-off errors since months are not uniform. As well this highly affects the computation of the approximate rate of consumption of nutrients.

Fig.4.4 gives the plots of experimental and simulation radius versus time in months. There is weak convergence particularly on the extremes which is attributed to the rounding off errors as highlighted in above paragraph.

In order to obtain the results in days, equation (4.4) need to be formulated as;

$$\frac{\partial C}{\partial t} = \frac{x^2}{8760} C_{xx} + \lambda x^4 \quad \text{.....(4.20)}$$

Where proportionality constant (D_C) is approximated as a ratio of 1 hour/ 1 year, an year being taken as a period of approximately 365 days.

Solving equation (4.20) by ADM provide the series (4.21) below

$$C(x,t) = \lambda x^4 (t + \frac{t^2}{1460} + \frac{t^3}{3.2\times10^6} + \frac{t^4}{9.3\times10^9} + \frac{t^5}{3.4\times10^{13}} + ----- \text{.....(4.21)}$$

Results generated from equation (4.21) and ones obtained from medical literature are as tabulated.

Table 4.5: Comparison between experimental and simulation radius in days.

Time in Days	***Experimental Radius(mm)***	***Simulation Radius (mm)***	***Absolute Error (mm)***	***%(Error/ Experimental Radius)***
250	*8.0*	*9.0*	*1.0*	*12.5*
280	*10.5*	*10.3*	*0.2*	*1.9*
310	*12.0*	*11.6*	*0.4*	*3.3*
345	*13.5*	*13.3*	*0.2*	*1.5*
375	*15.0*	*14.8*	*0.2*	*1.3*
415	*16.5*	*16.8*	*0.3*	*1.8*
454	*18.5*	*19.0*	*0.5*	*2.7*
507	*22.0*	*22.1*	*0.1*	*0.5*
560	*25.0*	*25.4*	*0.4*	*1.6*
625	*30.0*	*29.8*	*0.2*	*0.7*

Fig.4.5: Experimental and simulation radius against time in days.

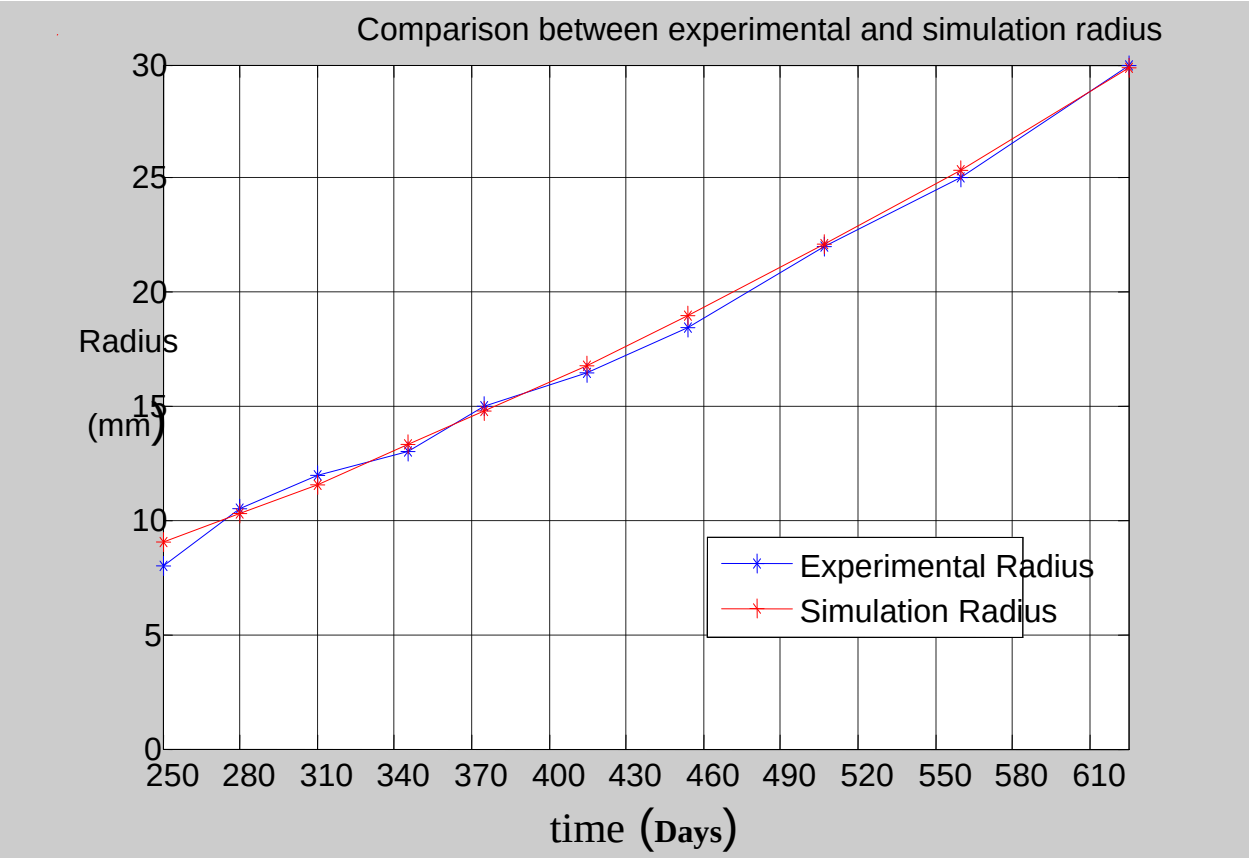

Table 4.5 gives comparison between experimental and simulation radius against time in days. Results obtained in days from one dimensional model are very realistic since they compare well with the experimental ones. Taking the year to be approximately 365 days, then it is possible to obtain good approximations for the simulation in this specific model.

Fig.4.5 gives the plots of experimental and simulation radius versus time in days. The two curves reflect good convergence.

Numerical simulation using Finite Volume Method.

In this case the one dimensional model is divided into small volumes within the domain of 250 to 560 days since reaction diffusion model is only viable after vascularization. Finite volume method is applied by integrating the equation over controlled volumes. The discretized equations are derived and finally, numerical simulation is obtained so as to demonstrate the convergence of the two methods.

Equation (4.4) can be presented as;

$$\frac{\partial \phi}{\partial t} = \frac{x_p^2}{24}\frac{\partial^2 \phi}{\partial x^2} + x_p^4 \quad \text{.....(4.22)}$$

Where ϕ is the variable for nutrients concentration.

x and t are variables for space and time respectively.

x_p defines the nodal points.

Where $\phi(x,0) = \phi_0 = 0$ is the initial condition, that is, at $t = 0$, technically it is assumed that there is no spheroid.

Applying finite volume method on equation (4.22) then the discretized equations obtained are;

$$1.27\phi_1 + \phi_2 = 22.67$$

$$-2816.67\phi_1 + 3000\phi_2 + 1166.67\phi_3 = 81$$

$$-10.93\phi_2 + 13.33\phi_3 - 2.4\phi_4 = 1$$

$$-650\phi_3 + 980\phi_4 - 330\phi_5 = 144$$

$$-323.33\phi_4 + 540\phi_5 - 216.67\phi_6 = 131.2$$

$$-1370\phi_5 + 2420\phi_6 - 1050\phi_7 = 878.4$$

$$-1850\phi_6 + 3380\phi_7 - 1530\phi_8 = 1713.6$$

$$-32.13\phi_7 + 60\phi_8 - 27.87\phi_9 = 40.5$$

$$-3050\phi_8 + 5780\phi_9 - 2730\phi_{10} = 5011.2$$

$$-160\phi_8 - 3770\phi_9 + 10830\phi_{10} = 172500.81 \quad \text{.....(4.23)}$$

Solving the discretized equations (4.23) by MATLAB provides the results tabulated below under the FVM Column.

The table below gives the solutions obtained from equation (4.4) by both ADM and FVM.

Table 4.6: Comparison between experimental and simulation radius via ADM and FVM.

Time in Days	*Experimental Radius(mm)*	*ADM Simulation (mm)*	*Error (mm)*	*% Error*	*FVM Simulation (mm)*	*Error (mm)*	*% Error*
250	*8.0*	*9.0*	*1.0*	*12.5*	*7.8*	*0.2*	*2.5*
280	*10.5*	*10.3*	*0.2*	*1.9*	*8.2*	*2.3*	*21.9*
310	*12.0*	*11.6*	*0.4*	*3.3*	*9.8*	*2.2*	*18.3*
345	*13.5*	*13.3*	*0.2*	*1.5*	*12.4*	*1.1*	*8.1*
375	*15.0*	*14.8*	*0.2*	*1.3*	*15.7*	*0.7*	*4.7*
415	*16.5*	*16.8*	*0.3*	*1.8*	*19.1*	*2.6*	*15.8*
454	*18.5*	*19.0*	*0.5*	*2.7*	*22.2*	*3.7*	*20.0*
507	*22.0*	*22.1*	*0.1*	*0.5*	*24.2*	*2.2*	*10.0*
560	*25.0*	*25.4*	*0.4*	*1.6*	*24.7*	*0.3*	*1.2*

Fig. 4.6: Experimental and simulation radius in both ADM and FVM against time in days.

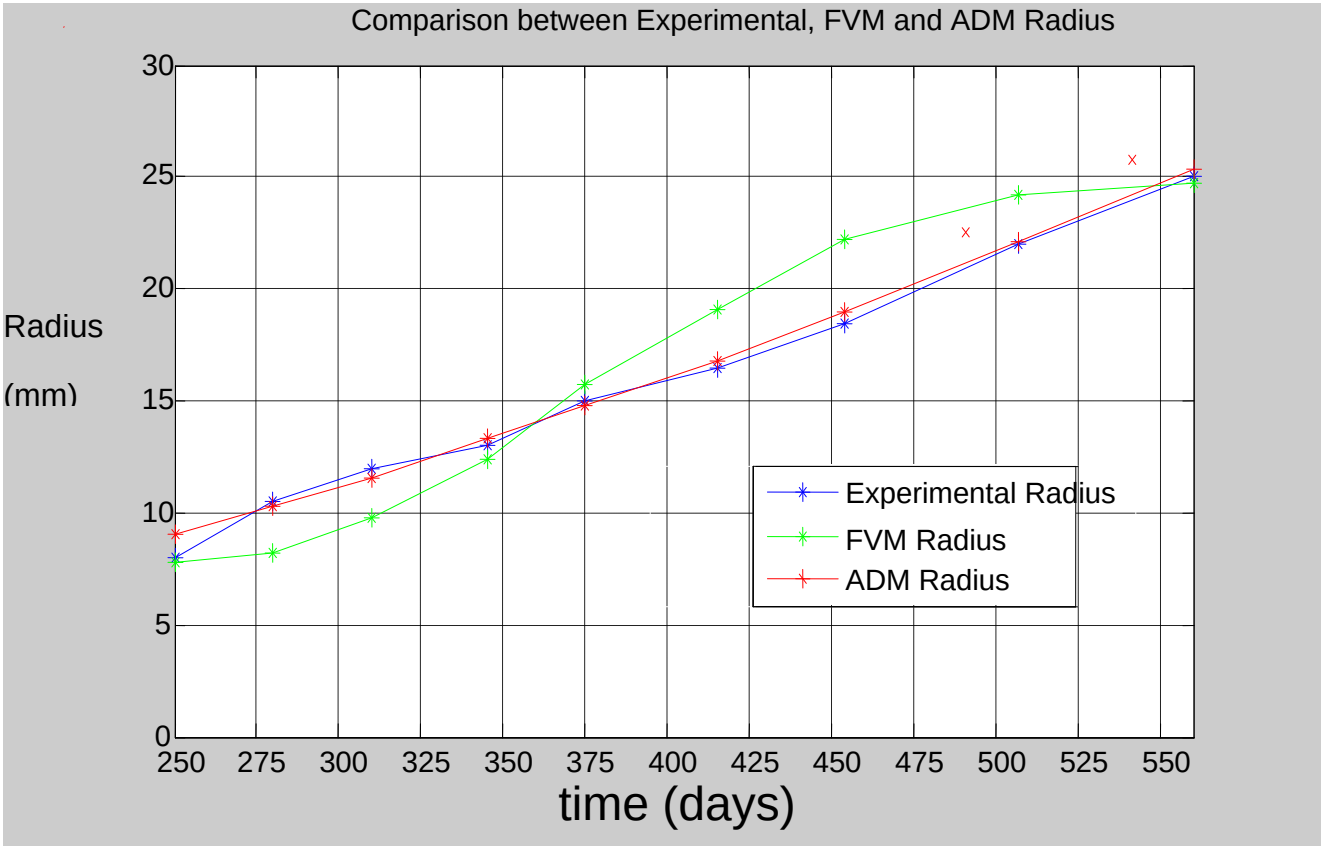

Table 4.6 gives comparison between experimental and simulation radius against time in days. Results obtained via ADM are more realistic than those obtained via FVM since they compare well with the experimental ones. ADM gives better approximations for the simulation in this specific model.

Fig.4.6 gives the plots of experimental and simulation radius both in ADM and FVM versus time in days. ADM reflect better convergence than FVM.

4.2: Two dimensional models.

This section gives the simulation procedure, results and discussion for two dimensional models which provides the tumor cross sectional area at selected time points. Results obtained are validated by comparing them with analytical results obtained by extrapolating the radius.

With mass conservation applied to the cells, the set of equations governing the evolution of proliferating, non- proliferating, necrotic cells densities and also nutrients access from underlying tissues in two dimensions can be developed from one dimensional model for Sheralt and Chaplain (2001) to give;

$$\frac{\partial P}{\partial t} = \frac{\partial}{\partial x}\left[\frac{P}{P+P_n}\frac{\partial (P+P_n)}{\partial x}\right] + \frac{\partial}{\partial y}\left[\frac{P}{P+P_n}\frac{\partial (P+P_n)}{\partial y}\right] + mP - nP - qP. \quad \text{…..…..…..…….(4.24)}$$

$$\frac{\partial P_n}{\partial t} = \frac{\partial}{\partial x}\left[\frac{P_n}{P+P_n}\frac{\partial (P+P_n}{\partial x}\right] + \frac{\partial}{\partial y}\left[\frac{P_n}{P+P_n}\frac{\partial (P+P_n}{\partial y}\right] + mP - rP_n$$

…….……...….(4.25)

$$\frac{\partial n}{\partial t} = rP_n. \quad \text{…….……...……..……..…..(4.26)}$$

$$\frac{\partial C}{\partial t} = D_c\left\{x^2\frac{\partial^2 C}{\partial x^2} + y^2\frac{\partial^2 C}{\partial y^2}\right\} + \Gamma f(x,y) \quad \text{……...……...…...…...……(4.27)}$$

Where:

D_C and Γ are positive constants.

mP ; reprsents mitosis rate of the proliferating cells .

nP; represents the rate at which proliferating cells becomes non – proliferative.

qP; represents the growth retardation rate.

rP_n; Represents the rate at which non-proliferative cells which are completely deprived of nutrients undergo necrosis.

Equation (4.27) represents the access of nutrients from underlying tissues

This is the equation of interest in this work, whereby

Proportionality constant (D_C) is approximated as a ratio of 2 hours/ 1 day and $\Gamma f(x, y)$ is the nutrients consumption rate in two dimensions, hence the exact model for simulation in two dimensions becomes;

$$\frac{\partial C}{\partial t} = \frac{x^2}{12} C_{xx} + \frac{y^2}{12} C_{yy} + \Gamma x^4 y^4 \qquad \text{.....(4.28)}$$

Applying the inverse operator L^{-1} to both sides of equation (4.28) where $C(x, y.0) = 0$ is the initial condition, yields;

$$L_t^{-1} C(x, y, t) = L_t^{-1} \Gamma x^4 y^4 + \frac{1}{12} L_t^{-1} (x^2 C_{xx} + y^2 C_{yy})$$

$$C_0(x, y, t) = \Gamma x^4 y^4 t \qquad \text{.....(4.29)}$$

$$C_1(x, y, t) = \frac{1}{12} L_t^{-1} \{x^2 (C_0)_{xx} + y^2 (C_0)_{yy}\}$$

$$= \Gamma x^4 y^4 t^2 \quad \text{……(4.30)}$$

$$C_2(x,y,t) = \frac{1}{12} L_t^{-1}\{x^2 (C_1)_{xx} + y^2 (C_1)_{yy}\}$$

$$= \frac{2}{3} \Gamma x^4 y^4 t^3 \quad \text{……(4.31)}$$

$$C_3(x,y,t) = \frac{1}{12} L_t^{-1}\{x^2 (C_2)_{xx} + y^2 (C_2)_{yy}\}$$

$$= \frac{\Gamma x^4 y^4 t^4}{6} \quad \text{……(4.32)}$$

$$C_4(x,y,t) = \frac{1}{12} L_t^{-1}\{x^2 (C_3)_{xx} + y^2 (C_3)_{yy}\}$$

$$= \frac{\Gamma x^4 y^4 t^5}{15} \quad \text{……(4.33)}$$

$$C_5(x,y,t) = \frac{1}{12} L_t^{-1}\{x^2 (C_4)_{xx} + y^2 (C_4)_{yy}\}$$

$$= \frac{\Gamma x^4 y^4 t^6}{45} \quad \text{……(4.34)}$$

$$C_6(x,y,t) = \frac{1}{12} L_t^{-1}\{x^2 (C_5)_{xx} + y^2 (C_5)_{yy}\}$$

$$= \frac{2}{315} \Gamma x^4 y^4 t^7 \quad \text{……(4.35)}$$

$$C_7(x,y,t)=\frac{1}{12}L_t^{-1}\{x^2(C_6)_{xx}+y^2(C_6)_{yy}\}$$

$$=\frac{\Gamma x^4y^4t^8}{630}$$ ……………………………………………………………………….(4.36)

$$C_8(x,y,t)=\frac{1}{12}L_t^{-1}\{x^2(C_7)_{xx}+y^2(C_7)_{yy}\}$$

$$=\frac{\Gamma x^4y^4t^9}{2835}$$ ……………………………………………………………………….(4.37)

$$C_9(x,y,t)=\frac{1}{12}L_t^{-1}\{x^2(C_8)_{xx}+y^2(C_8)_{yy}\}$$

$$=\frac{\Gamma x^4y^4t^{10}}{14175}$$ ……………………………………………………………………….(4.38)

$$C_{10}(x,y,t)=\frac{1}{12}L_t^{-1}\{x^2(C_9)_{xx}+y^2(C_9)_{yy}\}$$

$$=\frac{2}{155925}\Gamma x^4y^4t^{11}$$ ……………………………………………………………………….(4.39)

$$C_{11}(x,y,t)=\frac{1}{12}L_t^{-1}\{x^2(C_{10})_{xx}+y^2(C_{10})_{yy}\}$$

$$=\frac{\Gamma x^4y^4t^{12}}{467775}$$ ……………………………………………………………………….(4.40)

.

$$C_n(x,y,t)=\frac{1}{12}L_t^{-1}\{x^2(C_{n-1})_{xx}+y^2(C_{n-1})_{yy}\}$$

.

……………………………………….(4.41)

In this model ADM generates the solution in series of the form;

$$C(x,y,t) = C_0(x,y,t) + C_1(x,y,t) + C_2(x,y,t) + C_3(x,y,t) + \ldots\ldots\ldots\ldots + C_n(x,y,t) \quad \ldots\ldots\ldots\ldots(4.42)$$

Where

$$\lim_{n\to\infty} C_n(x,y,t) \to 0$$

Therefore from equation (4.29) to (4.41), the solution in a series form is given by;

$$C(x,y,t) = \Gamma x^4 y^4 (t + t^2 + \frac{2}{3}t^3 + \frac{t^4}{6} + \frac{t^5}{15} + \frac{t^6}{45} + \frac{2}{315}t^7 + \frac{t^8}{630} + \frac{t^9}{2835} + \frac{t^{10}}{14{,}175} + - - -) \quad \ldots(4.43)$$

Where $C(x,y,t)$ is the level of nutrients concentration in two dimensions which gives the cross section area of the tumor. Taking $\Gamma x^4 y^4$ as the rate of consumption of the nutrients and t as variable for time at selected points, then equation (4.43) generate the results given in the tables below.

The table below gives the results for two dimensional models at $\Gamma x^4 y^4 = 1.21 cm^2 / year$**.**

Taking $\Gamma x^4 y^4 \approx \Gamma x^4$ that is $1.21\, cm^2 / year$ as the rate of consumption of the nutrients in two dimensions, results generated from equation (4.43) alongside the analytical ones are tabulated below.

Table 4.7: Comparison between analytical and simulation cross section area at $\Gamma x^4 y^4 = 1.21 cm^2 / year$

Time in Days	***Analytical Cross section Area (cm^2)***	***Simulation Cross section Area (cm^2)***	***Absolute Error (cm^2)***	***%{error/Analytical area}***
280	*3.47*	*2.10*	*1.37*	*39.5*
310	*4.52*	*2.55*	*1.97*	*43.6*
345	*5.73*	*3.16*	*2.57*	*44.9*
375	*7.07*	*3.75*	*3.32*	*47.0*
415	*8.56*	*4.69*	*3.87*	*45.2*
454	*10.76*	*5.81*	*4.95*	*46.0*
507	*15.21*	*7.65*	*7.56*	*49.7*
560	*19.64*	*10.01*	*9.63*	*49.0*
625	*28.29*	*13.82*	*14.47*	*51.1*

Fig. 4.7: Analytical and simulation cross section area against time in days a $\Gamma x^4 y^4 = 1.21 cm^2 / year$.

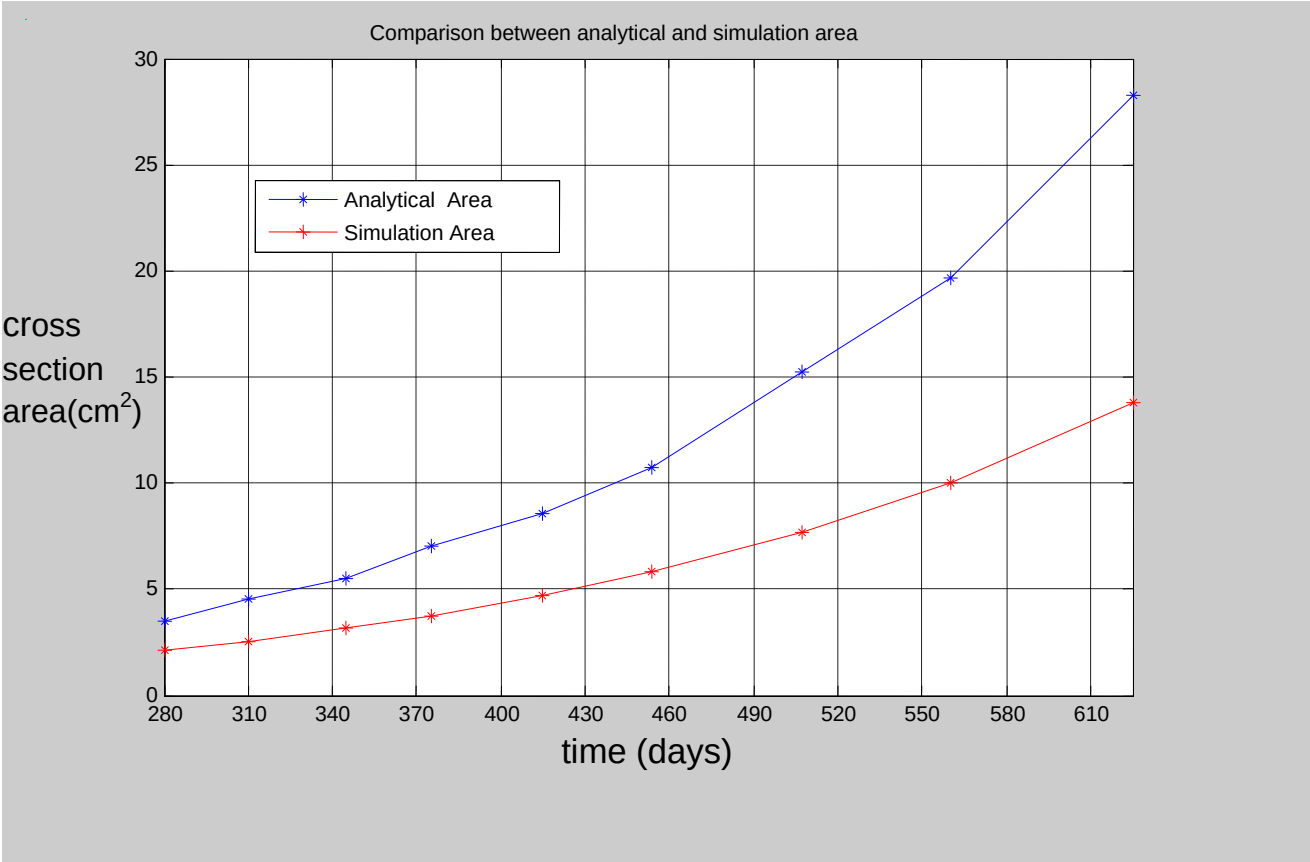

Table 4.7 gives the comparison between analytical and simulation cross section area where the rate of consumption of the nutrients in two dimensions is assumed to be 1.21cm^2/year. The model provides unrealistic results owing to the percentage error reflected at selected time points. It is observed that two dimensional model is not viable at this rate of nutrients consumption.

Fig.4.7 gives the plots of analytical and simulation cross section area against time in days. The model fails to converge at this rate of nutrients consumption.

The table below gives the results for two dimensional model at $\Gamma x^4 y^4 = 2.3 cm^2 / year$.

Taking $\Gamma x^4 y^4 \approx 2\lambda x^4$ as the rate of consumption of the nutrients in two dimensions, results generated from equation (4.43) alongside the analytical ones are tabulated below.

Table 4.8: Comparison between analytical and simulation cross section area at $\Gamma x^4 y^4 = 2.3 cm^2 / year$

Time in Days	***Analytical Cross section Area (cm^2)***	***Simulation Cross section Area (cm^2)***	***Absolute Error (cm^2)***	***%(Error/ Analytical Area)***
280	*3.46*	*4.00*	*0.54*	*15.6*
310	*4.52*	*4.85*	*0.33*	*7.3*
345	*5.73*	*6.00*	*0.27*	*4.7*
375	*7.07*	*7.13*	*0.06*	*0.9*
415	*8.56*	*8.92*	*0.36*	*4.2*
454	*10.76*	*11.04*	*0.28*	*2.6*
507	*15.21*	*14.54*	*0.67*	*4.4*
560	*19.64*	*19.02*	*0.62*	*3.2*
625	*28.29*	*26.27*	*2.02*	*7.1*

Fig.4.8: Analytical and simulation cross section area against time in days at $\Gamma x^4 y^4 = 2.3cm^2 / year$.

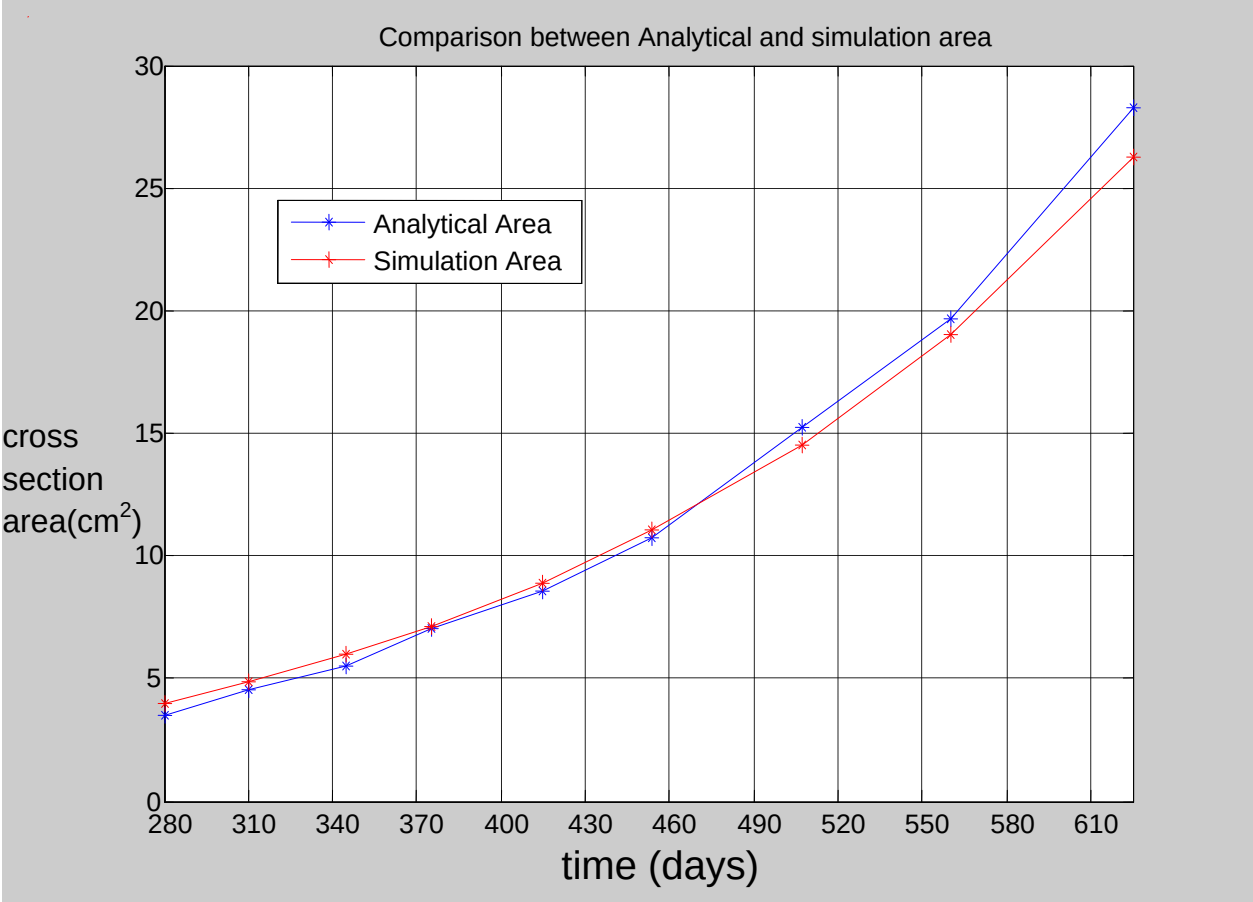

Table 4.8 gives comparison between analytical and simulation cross section area where the rate of consumption of the nutrients is assumed to be 2.3cm^2/year. The tumor is already vascularized and the model provides realistic results. It is observed that 2.3cm^2 /year is the viable rate of nutrients consumption in two dimensional model since 67% of the values are within the confidence level.

Fig. 4.8 gives the plots of analytical and simulation cross section area against time in days.

The obtained simulations undergoes high variations as the region becomes wide which can be attributed to the instability of the method (ADM) since it has weak stability on wide regions.

The table below gives the results for two dimensional model at $\Gamma x^4 y^4 = 2.4 cm^2 / year$.

Taking $\Gamma x^4 y^4 > 2\lambda x^4$ that is $2.4 cm^2 / year$ as the rate of consumption of the nutrients. Results generated from equation (4.43) alongside the analytical ones are as tabulated below.

Table 4.9: Comparison between analytical and simulation cross section area at $\Gamma x^4 y^4 = 2.4 cm^2 / year$

Time in Days	***Analytical Cross section Area (cm^2)***	***Simulation Cross section Area (cm^2)***	***Absolute Error (cm^2)***	***%(Error/ Analytical Area)***
280	*3.46*	*4.17*	*0.71*	*20.5*
310	*4.52*	*5.06*	*0.54*	*11.9*
345	*5.73*	*6.26*	*0.53*	*9.2*
375	*7.07*	*7.44*	*0.37*	*5.2*
415	*8.56*	*9.31*	*0.75*	*8.8*
454	*10.76*	*11.52*	*0.76*	*7.1*
507	*15.21*	*15.17*	*0.04*	*0.3*
560	*19.64*	*19.85*	*0.21*	*1.1*
625	*28.29*	*27.41*	*0.88*	*3.1*

Fig. 4.9: Analytical and simulation area against time in days at $\Gamma x^4 y^4 = 2.4cm^2 / year$

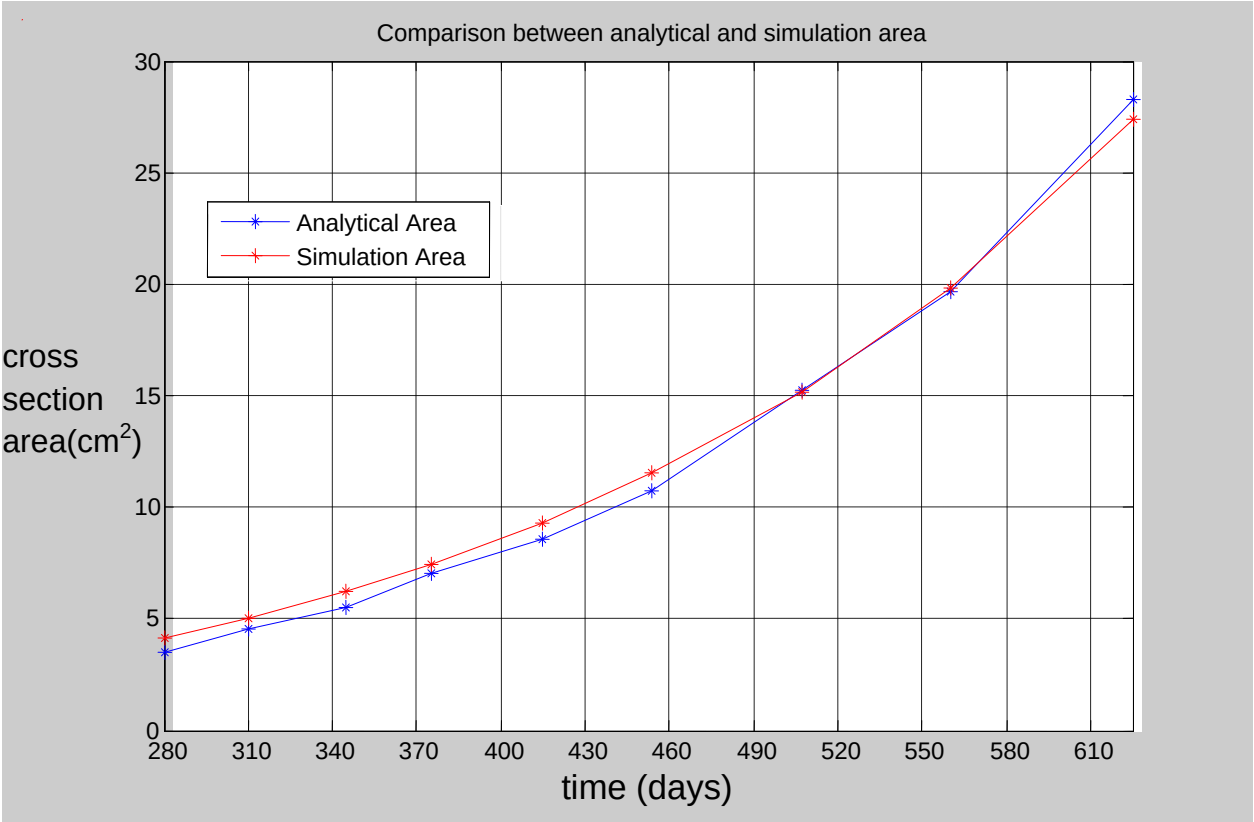

Table 4.9 gives comparison between analytical and simulation cross section area where the rate of consumption of the nutrients is assumed to be 2.4cm^2/year. Simulation provides unrealistic results since 67% of the values are outside the confidence level hence $\Gamma x^4 y^4 \geq 2.4cm^2 / year$ is not a viable rate of nutrients consumption in the two dimensional model.

Fig. 4.9 gives the plots of analytical and simulation cross section area against time in days. The obtained simulation fails to converge well in the lower stages of tumor growth and development which can be attributed to high rate of consumption of the nutrients.

4.3: Three dimensional models.

This section gives the simulation procedure, results and discussion for three dimensional models which provides the tumor volume at selected time points. Results obtained are validated by comparing them with the analytical results obtained by extrapolating the radius.

With mass conservation applied to the cells, the set of equations governing the evolution of proliferating, non- proliferating, necrotic cells densities and also nutrients access from underlying tissues in three dimensions can be developed from one dimensional model for Sheralt and Chaplain (2001) to give ;

$$\frac{\partial P}{\partial t}=\frac{\partial}{\partial x}\left[\frac{P}{P+P_n}\frac{\partial(P+P_n)}{\partial x}\right]+\frac{\partial}{\partial y}\left[\frac{P}{P+P_n}\frac{\partial(P+P_n)}{\partial y}\right]+\frac{\partial}{\partial z}\left[\frac{P}{P+P_n}\frac{\partial(P+P_n)}{\partial z}\right]+sP-tP-uP\ldots(4.44)$$

$$\frac{\partial P_n}{\partial t}=\frac{\partial}{\partial x}\left[\frac{P_n}{P+P_n}\frac{\partial(P+P_n}{\partial x}\right]+\frac{\partial}{\partial y}\left[\frac{P_n}{P+P_n}\frac{\partial(P+P_n}{\partial y}\right]+\frac{\partial}{\partial z}\left[\frac{P_n}{P+P_n}\frac{\partial(P+P_n}{\partial z}\right]+sP-vP_n$$

$\ldots\ldots\ldots\ldots\ldots\ldots\ldots\ldots\ldots\ldots\ldots\ldots\ldots\ldots\ldots\ldots\ldots\ldots\ldots\ldots\ldots\ldots\ldots\ldots\ldots\ldots\ldots\ldots\ldots\ldots\ldots\ldots\ldots\ldots\ldots\ldots$(4.45)

$$\frac{\partial n}{\partial t}=vP_n. \quad \ldots\ldots\ldots\ldots\ldots\ldots\ldots\ldots\ldots\ldots\ldots\ldots\ldots\ldots\ldots\ldots\ldots\ldots\ldots\ldots\ldots\ldots\ldots\ldots\ldots\ldots(4.46)$$

$$\frac{\partial C}{\partial t}=D_C\left\{x^2\frac{\partial^2 C}{\partial x^2}+y^2\frac{\partial^2 C}{\partial y^2}+z^2\frac{\partial^2 C}{\partial z^2}\right\}+\beta\ f(x,y,z) \quad \ldots\ldots\ldots\ldots\ldots\ldots\ldots\ldots\ldots\ldots\ldots(4.47)$$

Where;

D_C and β are positive constants.

sP ; reprsents mitosis rate of the proliferating cells

tP; represents the rate at which proliferating cells becomes non – proliferative

uP; represents the growth retardation rate

vP_n; Represents the rate at which non-proliferative cells which are completely deprived of nutrients undergo necrosis.

Equation (4.47) represents the access of nutrients from underlying tissues.

This is the equation of interest in this work, whereby

D_C is the proportionality constant and $\beta\ f(x,y,z)$ represents the nutrients consumption rate after the process of angiogenesis has taken place.

A proportionality constant of 3 hours/ 1 day is very high hence creating weakness in convergence of the model. By taking the constant as 2 hours/ 1 day, then the exact model for simulation in three dimensions becomes

$$\frac{\partial C}{\partial t} = \frac{1}{12}(x^2 C_{xx} + y^2 C_{yy} + z^2 C_{zz}) + \beta x^4 y^4 z^4 \quad \text{.....(4.48)}$$

Applying the inverse operator L^{-1} to both sides of equation (4.48) where $C(x,y.z,0) = 0$ is the initial condition, yields;

$$C(x,y,z,t) = \beta L_t^{-1} x^4 y^4 z^4 + \frac{1}{12} L_t^{-1}(x^2 C_{xx} + y^2 C_{yy} + z^2 C_{zz})$$

$$C_0(x,y,z,t) = \beta x^4 y^4 z^4 t \qquad \text{.....(4.49)}$$

$$C_1(x,y,z,t) = \frac{1}{12} L_t^{-1}\{x^2(C_0)_{xx} + y^2(C_0)_{yy} + z^2(C_0)_{zz}\}$$

$$= \frac{3\beta}{2} x^4 y^4 z^4 t^2 \qquad \text{.....(4.50)}$$

$$C_2(x,y,z,t) = \frac{1}{12} L_t^{-1}\{x^2(C_1)_{xx} + y^2(C_1)_{yy} + z^2(C_1)_{zz}\}$$

$$= \frac{3\beta}{2} x^4 y^4 z^4 t^3 \qquad \text{.....(4.51)}$$

$$C_3(x,y,z,t) = \frac{1}{12} L_t^{-1}\{x^2(C_2)_{xx} + y^2(C_2)_{yy} + z^2(C_2)_{zz})$$

$$= \frac{9\beta}{8} x^4 y^4 z^4 t^4 \qquad \text{.....(4.52)}$$

$$C_4(x,y,z,t) = \frac{1}{12} L_t^{-1}\{x^2(C_3)_{xx} + y^2(C_3)_{yy} + z^2(C_3)_{zz}\}$$

$$= \frac{27\beta}{40} x^4 y^4 z^4 t^5 \qquad \text{.....(4.53)}$$

$$C_5(x,y,z,t) = \frac{1}{12} L_t^{-1}\{x^2(C_4)_{xx} + y^2(C_4)_{yy} + z^2(C_4)_{zz}\}$$

$$= \frac{27\beta}{80} x^4 y^4 z^4 t^6 \qquad \text{.....(4.54)}$$

$$C_6(x,y,z,t) = \frac{1}{12} L_t^{-1}\{x^2(C_5)_{xx} + y^2(C_5)_{yy} + z^2(C_5)_{zz}\}$$

$$= \frac{81\beta}{560} x^4 y^4 z^4 t^7 \quad \text{……(4.55)}$$

$$C_7(x,y,z,t) = \frac{1}{12} L_t^{-1}\{x^2(C_6)_{xx} + y^2(C_6)_{yy} + z^2(C_6)_{zz}\}$$

$$= \frac{243\beta}{4480} x^4 y^4 z^4 t^8 \quad \text{……(4.56)}$$

$$C_8(x,y,z,t) = \frac{1}{12} L_t^{-1}\{x^2(C_7)_{xx} + y^2(C_7)_{yy} + z^2(C_7)zz\}$$

$$= \frac{81\beta}{4480} x^4 y^4 z^4 t^9 \quad \text{……(4.57)}$$

$$C_9(x,y,z,t) = \frac{1}{12} L_t^{-1}\{x^2(C_8)_{xx} + y^2(C_8)_{yy} + z^2(C_8)_{zz}\}$$

$$= \frac{243\beta}{44800} x^4 y^4 z^4 t^{10} \quad \text{……(4.58)}$$

$$C_{10}(x,y,z,t) = \frac{1}{12} L_t^{-1}\{x^2(C_9)_{xx} + y^2(C_9)_{yy} + z^2(C_9)_{zz}\}$$

$$= \frac{729\beta}{492,800} x^4 y^4 z^4 t^{11} \quad \text{……(4.59)}$$

$$C_{11}(x,y,z,t) = \frac{1}{12} L_t^{-1}\{x^2(C_{10})_{xx} + y^2(C_{10})_{yy} + z^2(C_{10})_{zz}\}$$

$$= 0.000369825 \ \beta x^4 y^4 z^4 t^{12} \quad \text{……(4.60)}$$

$$C_{12}(x,y,z,t)=\frac{1}{12}L_t^{-1}\{0.013313717\ x^4y^4z^4t^{12}\}$$

$$=0.0000853\ \beta x^4y^4z^4t^{13} \quad \text{……..……..…….....……..…(4.61)}$$

$$C_{13}(x,y,z,t)=\frac{1}{12}L_t^{-1}\{0.0030724\ x^4y^4z^4t^{13}\}$$

$$=0.00001839\ \beta x^4y^4z^4t^{14} \quad \text{…….……..…..…..…..……..(4.62)}$$

$$C_{14}(x,y,z,t)=\frac{1}{12}L_t^{-1}\{0.00658371x^4y^4z^4t^{14}\}$$

$$=0.00000366\ \beta x^4y^4z^4t^{15} \quad \text{……...……..……..……..……..…(4.63)}$$

$$C_n(x,y,z,t)=\frac{1}{12}L_t^{-1}\{x^2(C_{n-1})_{xx}+y^2(C_{n-1})_{yy}+z^2(C_{n-1})_{zz}\} \quad \text{……..……...…(4.64)}$$

In this model, ADM generates the solution in a series of the form;

$$C(x,y,z,t)=C_n(x,y,z,t)\ n=0,1,2\ldots\ldots \quad \text{……..…….(4.65)}$$

Whereby;

$$\lim_{n\to\infty}C_n(x,y,z,t)\to 0$$

Therefore from equation (4.49) to (4.64) the solution in a series form is given by;

$$C(x,y,z,t)=\beta x^4y^4z^4(t+\frac{3}{2}t^2+\frac{3}{2}t^3+\frac{9}{8}t^4+\frac{27}{40}t^5+\frac{27}{80}t^6+\frac{81}{560}t^7+\frac{243}{4480}t^8--) \quad \text{..(4.66),}$$

Where $C(x,y,z,t)$ is the level of nutrients concentration in three dimensions which gives the

volume of the tumor and $\beta x^4 y^4 z^4$ is the rate of consumption of the nutrients in three dimensions, developed from λx^4, which is the rate of nutrients consumption in one dimensional model and t is a variable for time at selected points then equation (4.66) generate the results given in the tables below.

The table below gives the results for three dimensional model at $\beta x^4 y^4 z^4 = 1.331 cm^3 / year$

Taking $\beta x^4 y^4 z^4 = (\lambda x^4)^3 = 1.331 cm^3 / year$ as the rate of nutrients consumption in three dimensions, then results generated from equation (4.66) alongside the analytical ones are as tabulated.

Table 4.10: Comparison between analytical and simulation volume at $\beta x^4 y^4 z^4 = 1.331 cm^3 / year$

Time in Days	***Analytical Volume (cm^3)***	***Simulation Volume (cm^3)***	***Absolute Error (cm^3)***	***% (Error/ Analytical volume)***
280	*4.85*	*3.99*	*0.86*	*17.7*
310	*7.24*	*5.22*	*2.02*	*27.9*
345	*10.31*	*7.11*	*3.20*	*31.0*
375	*14.14*	*9.22*	*4.92*	*34.8*
415	*18.82*	*12.99*	*5.83*	*31.0*
454	*26.53*	*18.08*	*8.45*	*31.9*
507	*43.41*	*28.18*	*15.23*	*35.1*
560	*65.48*	*43.78*	*21.70*	*33.1*
625	*113.14*	*74.99*	*38.15*	*33.7*

Fig. 4.10: Analytical and simulation volume against time in days at $\beta x^4 y^4 z^4 = 1.331 cm^3 / year$

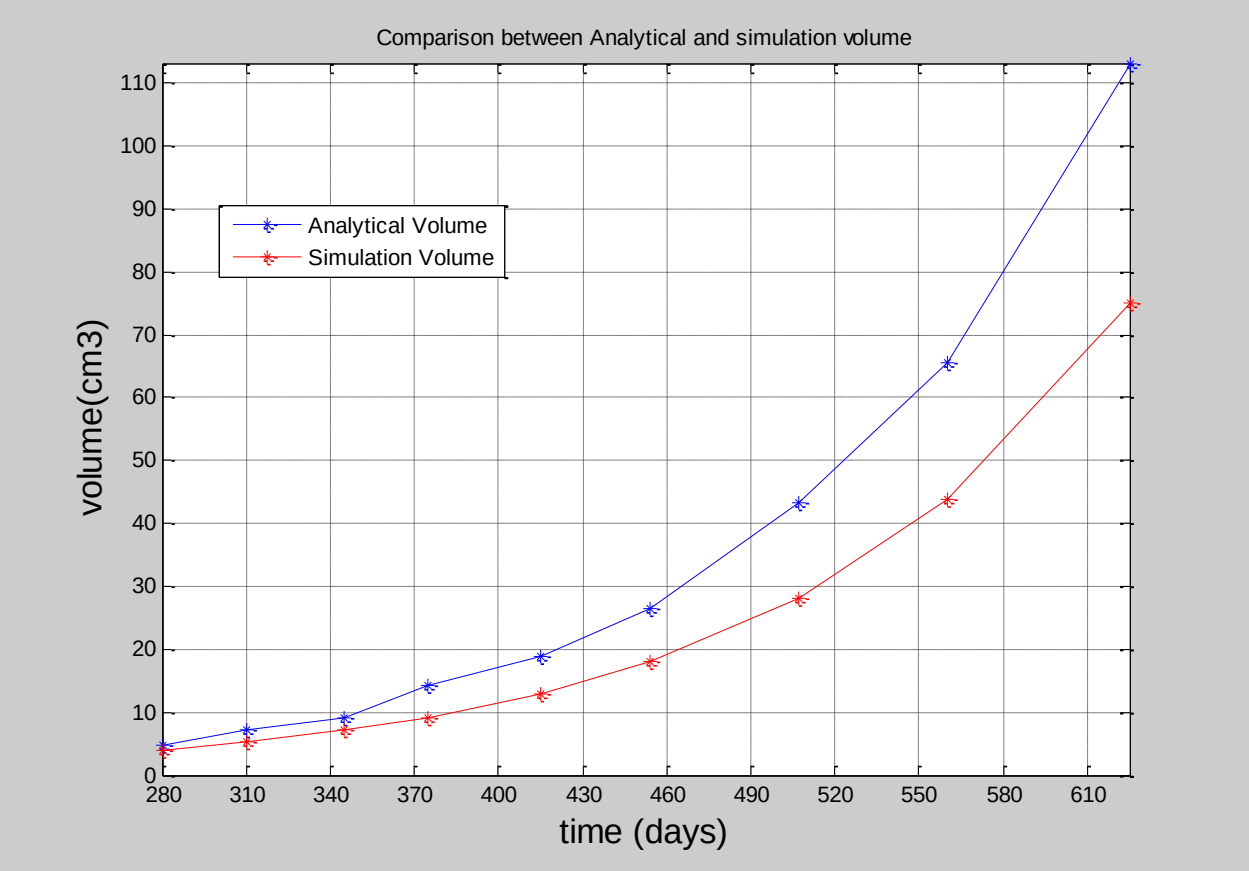

Table4.10 gives the comparison between analytical and simulation volume where the rate of nutrients consumption in three dimensions is assumed to be 1.331cm^3/year. The model provides unrealistic results as reflected at selected time points. It is observed that three dimensional model is not viable at this rate of nutrients consumption.

Fig. 4.10 gives the plots of analytical and simulation volume at $\beta x^4 y^4 z^4 = 1.331 cm^3 / year$. There is no convergence at this stage of vascularization once the rate of consumption of nutrients is 1.331cm^3/year.

The table below gives the results for three dimensional models at $\beta x^4 y^4 z^4 = 2.0 cm^3 / year$

Taking $\beta x^4 y^4 z^4 < 2\lambda x^4 = 2.0 cm^3 / year$ as the rate of consumption of the nutrients in three dimensions, results obtained from equation (4.66) alongside the analytical ones are as tabulated below.

Table 4.11: Comparison between analytical and simulation volume at $\beta x^4 y^4 z^4 = 2.0 cm^3 / year$

Time in Days	***Analytical Volume (cm^3)***	***Simulation Volume (cm^3)***	***Absolute Error (cm^3)***	***% (Error/ Analytical volume)***
280	*4.85*	*5.99*	*1.14*	*23.5*
310	*7.24*	*7.85*	*0.61*	*8.43*
345	*10.31*	*10.69*	*0.38*	*3.69*
375	*14.14*	*13.85*	*0.29*	*2.05*
415	*18.82*	*19.53*	*0.71*	*3.77*
454	*26.53*	*27.17*	*0.64*	*2.41*
507	*43.41*	*42.35*	*1.06*	*2.44*
560	*65.48*	*65.77*	*0.29*	*0.44*
625	*113.14*	*112.68*	*0.46*	*0.41*

Fig. 4.11: Analytical and simulation volume against time in days at $\beta x^4 y^4 z^4 = 2.0cm^3 / year$

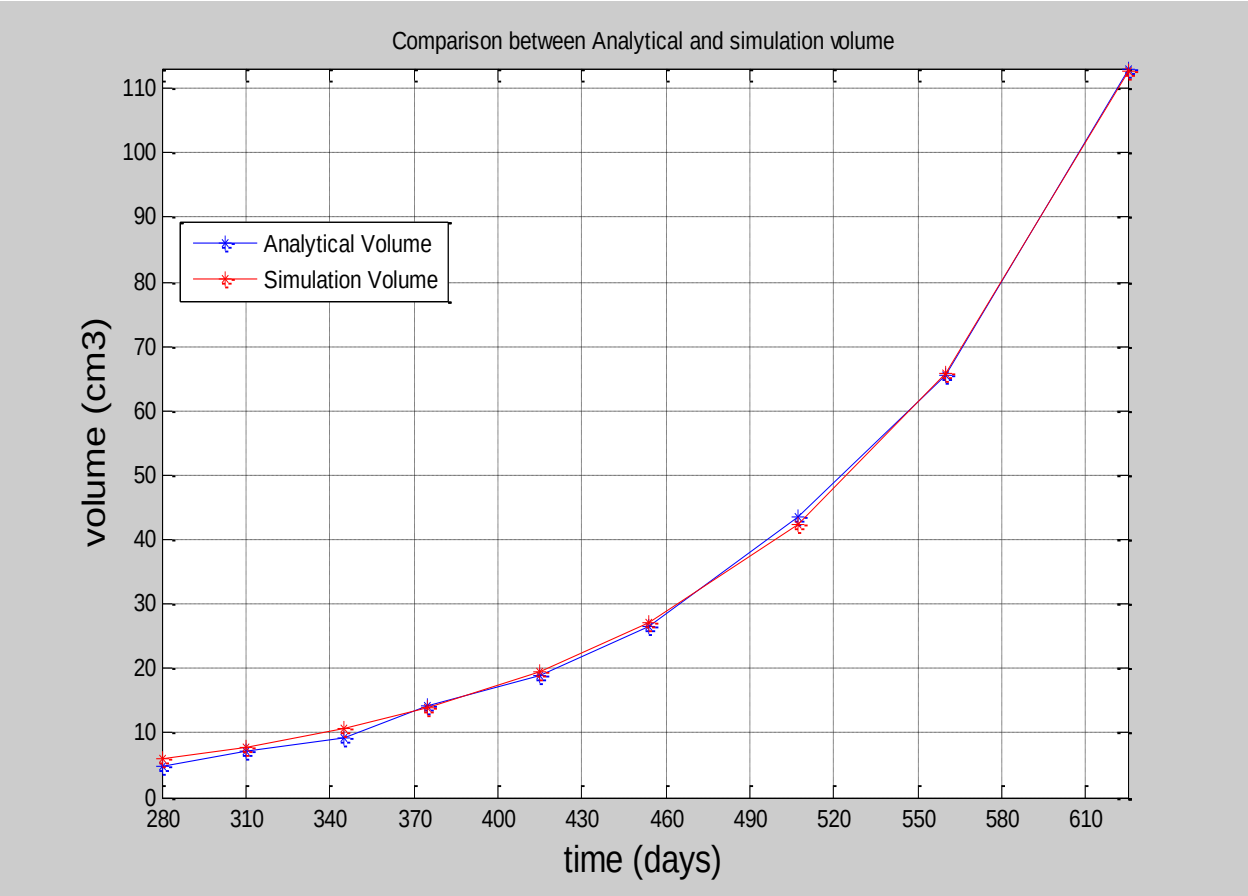

Table 4.11 gives the comparison between analytical and simulation volume where the rate of consumption of the nutrients is assumed to be 2.0cm^3/year. Analytical volume is obtained by extrapolating the radius.It is observed that simulation of three dimensional models provides very realistic results at most of the selected time points. Three dimensional models give better results than two dimensional models since 78% of the values obtained are within the confidence level. Generally, one dimensional model is the best in this work owing to its high level of convergence as well as realizing better results at 89% of the values obtained at the selected time points, nevertheless tumors are three dimensional objects hence three dimensional model give better approximations.

Fig. 4.11 gives the plots of analytical and simulation volume against time in days. Simulation in this model gives strong convergence.

The table below gives the results for three dimensional models at

$\beta x^4 y^4 z^4 = 2.1 cm^3 / year$ Taking $\beta x^4 y^4 z^4 = 2.1 cm^3 / year$ that is $> 2.0 cm^3 / year$ as the rate of consumption of the nutrients in three dimensions, then results generated from equation (4.66) alongside the analytical ones are as tabulated.

Table 4.12: Comparison between analytical and simulation volume at $\beta x^4 y^4 z^4 = 2.1 cm^3 / year$

Time in Days	***Analytical Volume (cm^3)***	***Simulation Volume (cm^3)***	***Absolute Error (cm^3)***	***% (Error/ Analytical volume)***
280	*4.85*	*6.29*	*1.44*	*29.7*
310	*7.24*	*8.23*	*0.99*	*13.7*
345	*10.31*	*11.22*	*0.91*	*8.8*
375	*14.14*	*14.55*	*0.41*	*2.9*
415	*18.82*	*20.50*	*1.68*	*8.9*
454	*26.53*	*28.53*	*2.00*	*7.5*
507	*43.41*	*44.46*	*1.05*	*2.4*
560	*65.48*	*69.08*	*3.6*	*5.5*
625	*113.14*	*118.31*	*5.17*	*4.6*

Fig.4.12: Analytical and simulation volume against time in days at $\beta x^4 y^4 z^4 = 2.1 cm^3 / year$

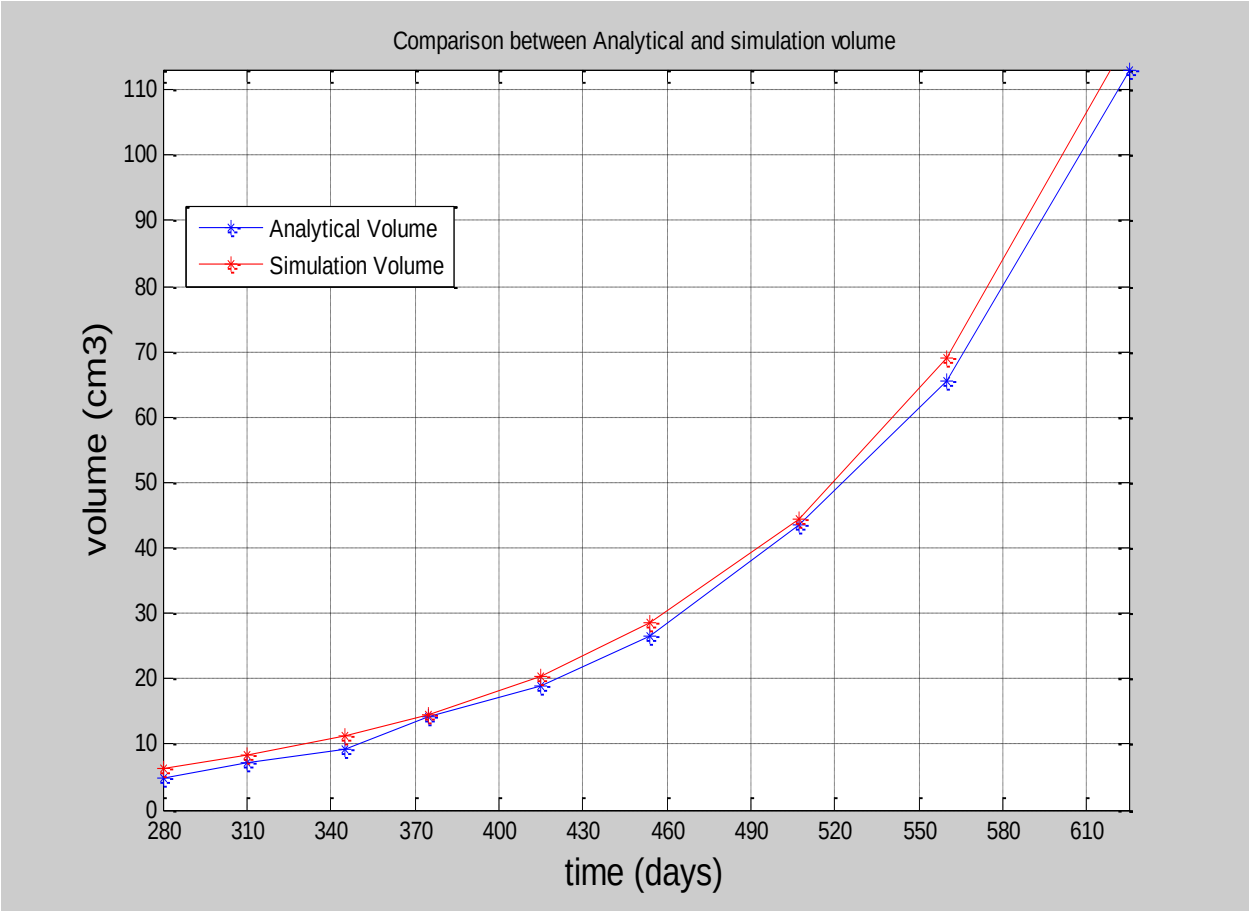

Table 4.12 gives the comparison between analytical and simulation volume where the rate of consumption of the nutrients is assumed to be 2.1cm^3/year. It is observed that an attempt to raise the rate of nutrients consumption will increase the volume at selected time points. This confirms that the only viable rate of nutrients consumption in this model is 2.0cm^3/year.

Fig. 4.12 gives the plots of analytical and simulation volume against time. Simulation in this model fails to converge owing to high rate of nutrients consumption.

The next chapter gives concluding remarks and recommendations regarding this work.

CHAPTER FIVE

CONCLUSION AND RECOMMENDATIONS

5.1 Conclusion

The model presented in this work focuses on the quantitative description of the dynamics of vascular brain tumor growth. It can be concluded that;

(i) Diffusion in the brain function plays a very vital role in delivery of nutrients to the tissues{Nicholson (2001)}hence it can be concluded that growth and development of a tumor is governed by a diffusion model where concentration of the nutrients (C) is the dependent variable, x, y, z are spatial independent variables and t is the variable for time.

(ii)Viable rates of nutrients consumption were found to be;

(a) 1.1cm/year for one dimensional model since 89% of the values at selected time points were found to be within 95% degree of confidence.

(b) 2.3cm^2/ year for two dimensional model since 67% of the values at selected time points were found to be within 95% degree of confidence.

(c) 2.0 cm^3 / year for three dimensional model since 78% of the values at selected time points were found to be within 95% degree of confidence.

(iii) Results obtained from the simulation predict the dynamics of GBM tumor proliferation at selected time points and they are realistic since they compare well with the data obtained from the medical literature.

(iv) Angiogenic inhibitors, that is drugs taken to hinder the process of angiogenesis can only be viable within 250 days since after this period reaction diffusion model is viable meaning the tumor is already vascularized.

5.2 Recommendations

Based on the results of this research, it is recommended that;

(i) Medical practitioners be using the volume in approximating the size of tumors in place of radius since volume is more realistic as tumors are three dimensional objects.

(ii) ADM gives a series solution which must be truncated for practical applications. Although the series can be rapidly convergent in a small region, it has very slow convergence in the wider region and the truncated series solution is inaccurate in that region which restricts the application area of the method. Convergence of one dimensional model is faster than both two and three dimensional models.

(iii) Parabolic models are not viable in early stages of growth and development of GBM tumors.

(iv) For GBM tumors $R(t) \to \infty$ as $t \to \infty$ where R is the tumor radius and t is time which is practically unrealistic, hence further research is recommended on ADM so as to give the behavior of the tumor where angiogenesis fails to take place.

(v) While the results confirm that ADM is able to produce realistic simulations in idealized cases, research is recommended to illustrate whether it has the ability to give the simulations of models of more complex situations that is where there is multiple distinct tumor clones.

REFERENCES

Abbaoui, K. Cherruault, Y. (1995). New ideas for proving convergence of decomposition method. *Journal of Applied Mathematics and Computing*, 29, 103-108.

Adam, J. A. (1986).A simplified mathematical model of tumor growth.*Journal of Mathematics and Bioscience*, 81,229-242.

Adomian, G. (1980). Non linear stochastic operator equations. *Journal of Theoretical Biol*ogy 501-544.

Adomian, A. &Rach, D.(1992). Noise terms in decomposition series solution, *Journal of Theoretical Biol*ogy 61-64.

Adomian, G. (1994). *Solving Frontier problems of physics: the decomposition method* .Kluwer, Boston, MA.

Aminataei, A., Hosseini, S. (2007).The comparison of the stability of Adomian decomposition method with numerical methods of equation solution.*Journal ofApplied Mathematics and Computing*, 186 665-669.

Bellomo, N. & Monaco, R. (1985).A comparison between Adomian's decomposition methods and perturbation techniques for nonlinear random differential equations.*Journal ofApplied Mathematics and Computing*, 110 495-502.

Biazar, J., Gholami, M. &Ghanbari,B. (2009). Extracting a general iterative method from an Adomian decomposition method and comparing it to the variational iteration method. *Journal of Applied Mathematics and Computing*, 59622-628.

Byrne, H., Chaplain, J. (1994). Growth of necrotic Tumors in the presence and absence of inhibitors. *School of Mathematical sciences, University of Bath , United Kingdom, 130,151-181.*

Cheng, A. & Tan, L.S. (2005).An avascular tumor model with random variation.*8th ATCM conference proceedings*, 1,153-161.

Chiocca, E. Deisboeck, T. Harsh, G. Kansal, A. &Torquato, S. (2000). Simulated Brain Tumor Growth Dynamics Using a Three- Dimensional Cellular Automaton. *Journal of Theoretical Biol*ogy 203, 367-382

Dutching, W. &Vogelsaenger, T. (1985).Recent progress in modeling and simulation of three –dimensional tumor growth and treatment. *Journal of Bio systems*, 18, 79-91.

Emad, H. A. (2012). Computers and Mathematics with applications. *Journal of Applied Mathematics and Computing*, 1056-1065.

Emad, H. A. (2011). *Advances* in the ADM for solving two- point nonlinear boundary value problems with Neumann boundary conditions. *Journal of Theoretical Biol*ogy 1931-1934.

Francisco, J.T.(2015). *3-Dimensional in vivo brain tumor geometry Study by scaling analysis*.

Friedman, A. (2013). A partial Differential Equation model of metastasized prostatic cancer. J*ournal of Mathematics and Bio-sci*ence, 10 591-608.

Friedman, A. (2006). Cancer Models and Their Mathematical Analysis, *Lecture notes. Journal of Math*ematics, 1872, 223-246.

Grimes, DR., Kannan P., McIntyre A., Kavanagh A., Siddiky A., Wigfield S. (2016).The Role of Oxygen in Avascular Tumor Growth.*PLoS ONE 11(4): e0153692. doi:10.1371/journal.pone.0153692*

Hillen, T. & Painter, K. J. (2013). Mathematical modeling of glioma growth, *Journal of Theoretical Biol*ogy, 323,25-39

Hosseini, M., &Nasabzadeh H. (2006).Convergence of Adomian decomposition method. *Journal of applied Mathematics and Computing,* 182536- 543.

Konukoglu E. Clatz, O. Bondiau, P. Delignette, H. & Ayache, N. (2010) Extrapolation glioma invasion margin in brain magnetic resonance images. *Journal of Medical Image Analysis*, 14, 111-125

Kumar, M. & Singh, G.(2010).A collection of computational techniques for solving singular boundary value problems.*Journal of mathematics, Analytical and Application,* 127 288-297.

Surgical Resection Coupled with the Immune System Response to Neoplastic Cells. *Journal of Computing and Medicine*, 20-24.

Nicholson, C. (2001). Diffusion and related transport mechanisms in brain tissue. Journal of *Rep.Prog.phys.*64, 815-884.

Qi, A. Zheng, X. (1993). A Cellular automaton model of cancerous growth.*Journal of Theoretical and Biol*ogy 161,1-12

Rach, R. (1987). Adomian decomposition method and comparisons with Picard's method, *Journal of mathematics, Analytical and Appl*ied mathematics, (128), 480-483.

Sherratt, J.A. & Chaplain, M. A. J. (2001).A new mathematical model for avascular tumor growth, *Journal of Mathematics and Biology*, 43, 291-312.

Smolle, J. & Stettner, H. (1993).Computer simulation of tumor cell invasion by a stochastic growth model.*160, 63-72.*

Wanjau,P.,Gatheri, F., Awuor, K. (2016) Comparison of convergence of Adomian decomposition method and fourth order Runge-Kutta method, *Asian Journal of Mathematics and Computer Research,**13**(3): 152-161*.

Wazwaz, A. (1997). Necessary conditions for the appearance of noise terms in decomposition solution series. *Journal of Applied Mathematics and Computing*, 81, 265-274.

Wazwaz, A. (1999). A reliable modification of Adomian decomposition method. *Journal of Applied Mathematics and Computing,* 102, 77-86.

Wazwaz, A., El-Sayed, S. (2001).A new modification of the Adomian decomposition method for linear and nonlinear operators.*Journal of Applied Mathematics and Computing,* 122,393-405.

Wenhai, C. (2004). An algorithm for Adomian decomposition method. *Journal of Applied Mathematics,* 159 221-235.

Yucheng, L. (2009). Adomian decomposition method with orthogonal polynomials. *Applied Mathematics and Computing,* 49, 1268-1273.

APPENDIX

```
clf

XLOW =i.e. minimum along the x axis;

XINC = i.e. step size along the x direction;

XHIGH =i.e. maximum along the x axis;

YLOW = i.e. minimum along the y axis

YINC = i.e. step size along the y axis

YHIGH = i.e. maximum along the y axis

%

A = [i.e. column for the time]

%

B = [i.e. column for the experimental data]

%

C=[i.e. column for the simulation ]

% for k=1:11

%  A(k) = graph1(k,1);

%  B(k) = graph1(k,2);

%  C(k) = graph1(k,3);

% end

h=plot(A(:),B(:),'b-*');hold on

K=plot(A(:),C(:),'g-*');hold on

%m=plot(D(:),C(:),'b.');hold off

%h=plot(A(:),B(:),C(:),D(:))

xlabel('time (days)','FontSize',15)
```

```
ylabel('volume(cm3)','Fontsize',15)
grid
Title('Comparison btnexpt& simulation radius')
%
axis([XLOW XHIGH YLOW YHIGH])
%set(gca,'xtick', [YLOW:YINC:YHIGH])%..NOTE THESE ARE THE Y-VALUES, i.e.
cross-stream direction!
%set(gca,'ytick', [XLOW:XINC:XHIGH])%..NOTE THESE ARE THE X-VALUES, i.e.
streamwise direction!
%
set(gca,'xtick', [XLOW:XINC:XHIGH])%..NORMAL NOTATION
set(gca,'ytick', [YLOW:YINC:YHIGH])%..NORMAL NOTATION
```